A dynamic utility cycling model for energy and time expenditure calculation of a population of cyclists

by

S.S. Soethout

Project duration:	September 2023 – August 2024	
Thesis committee:	Dr. J.K. Moore,	TU Delft, supervisor
	Ir. C.M Schmidt,	TU Delft, supervisor
	Dr. V.L. Knoop,	TU Delft

TU Delft

Contents

A dynamic utility cycling model for energy and time expenditure of a population of cyclists

S.S. Soethout

Abstract

In this research a dynamic time and energy model is constructed to simulate free flow utility cycling. Using a Monte Carlo simulation and distributions of rider and bicycle characteristics a population of cyclists is modelled to find the difference in time and energy expenditure on six different bicycle routes. The riders use realistic like power inputs and braking behaviour based on the rider and the route characteristics. While travel times are almost always lower for all cyclists when comparing routes, there are cyclists for who a shorter route distance does not equal a lower energy expenditure. For simpler routes (less elevation difference, traffic lights and shorter distance) the standard deviation of both time and energy decreases, showing that slow cyclist have a relative higher gain. For e-bike users there is even almost no difference in energy expenditure between the six evaluated routes that have varying elevation, traffic signals and routing, while travel times show a similar trend as for regular bicycles. With this model difference in routes can be quantified in matters of time and energy expenditure for a population of cyclists giving an objective picture of the differences between routes, which can be a useful tool for city planning and evaluation of bicycle infrastructure.

Keywords: Bicycle, Energy, Time, Model

1 Introduction

Bicycle highways are bicycle infrastructure in Europe that connect cities and suburbs to make cycling a more attractive type of transport for commuters. There are multiple factors for cyclist that decide whether a person decides to use the bicycle as transport mode for utility purposes, or to use another mode of transport. The most important factor in this decision is the travel time [1], [2], which bicycle highways aim to reduce and therefore increase the amount people choosing cycling as mode of transport. However, the travel time of cyclists is depending on both the infrastructure and cyclists themselves. The speed, and therefore travel time, depend on the power the cyclists delivers combined with the resistances acting on the cyclists. Therefore the travel time cannot be seen a standalone quantification of the preference rate of a bicycle route. In cycling there is a trade-off between travel time and energy expenditure [3]. The energy the rider uses is equivalent to a measure of effort, higher efforts will make cycling less attractive as a mode of transport [2]. It is therefore important to quantify both the travel time and energy expenditure of cyclist. For that reason this research has as goal to develop a dynamic bicycle energy and time model to be able to compare different bicycle routes and have the ability to quantify the differences between routes. This way a comparison between planned alternatives can be made to choose the best route for cyclists, or as demonstrated in this research, a new planned route can be compared to the existing routes to find out if it is better. And if it is better, how much better in being attractive to cyclists in matter of time and energy expenditure.

The focus of the model is not on an individual cyclist, but rather on a population of bicycle users. This way the characteristics of different kind of bicycles and people can be taken into account and give a more complete view of the time and energy cost of the people who will actually ride on the bicycle

routes. These different type of bicycle users include a spectrum of young adults to elderly users who can use the bicycle as a way of transport for different purposes, such as work, hobbies, shops or other utilities. This population of cyclists is made up of a single free flow cyclist at the time, meaning that each simulation is of a single cyclist with no interaction with other road users and for each cyclist a new simulation is done. A Monte Carlo simulation is then executed to get simulations with different inputs drawn from input distributions, from each input distribution of an input parameter a value is drawn to make a combination of a cyclist and a bicycle that will be simulated. For every new simulation new parameter values are drawn to have new cyclist and bicycle characteristics. To summarize, the research goal is to make a model that can be used to evaluate planned and existing routes for time and energy expenditure based on a population of free flow cyclists. To show the working and possibilities of the model a case study is performed on six bicycle routes in the city of Den Haag where a new bicycle highway is planned.

2 Methodology

The core of the model is an integration over time to solve the initial value problem of Newton's 2$^{\text{nd}}$ law, it solves for speed and distance over time. The cyclist and the bike are represented together as a single point mass model, therefore all inner forces in the system of bicycle and rider are disregarded and only the external forces acting on the body are present. These forces consist of the propulsion force of the rider, which will propel the bike, and resistances consisting of air drag, rolling resistance, gravitational force and internal losses in the drivetrain. E-bikes are growing in numbers in the Netherlands and are especially used for medium distances such as commuting trips [4]. Therefore it is important to include electrical bikes in the model. E-bikes are defined as bicycles with electrical assistance that only provide power when the rider is pedalling, moreover the maximum power delivered is 250 W as per European legislation. No fully motorized or bicycles with a throttle will be included in this research. A list of all symbols used that are used in the rest of this paper is given in Table 1.

2.1 Power and speed choice of cyclists

2.1.1 Comfort speed

The propulsion force of the bicycle rider system is provided by the cyclist. However, in comparison to the racing cyclist models, utility cyclists do not use full power [5], [6]. They use only a portion of their maximum power to reduce fatigue and to avoid sweating too much [3]. The power, and therefore speed, can vary greatly between different people, because there are differences in the amount of power a person is willing to give. This human provided power can increase when terrain changes, people might want to use more power when climbing a hill than on a flat road for example. The baseline power produced by the rider in the model is taken as the critical power (P_c). This is the power that, without fatigue, a human could exert indefinitely due to it being purely aerobic. As described before, utility cyclist do not use their full power. Therefore this critical power is multiplied by a percentage pct_{human} to simulate sub critical power levels in the range that represents power outputs for low effort and low fatigue where conversations are still possible [6]. Fatigue is excluded in the model, because the routes are relatively short distance and fatigue will most likely not play a large roll on short distances, especially when not using full power. This base power is used to calculate the comfort speed and represents the power the cyclist prefers to ride with at all times.

$$F_r = c_r m_{tot} g sin(\alpha) \tag{1a}$$

$$F_d = \frac{1}{2} A c_d \rho_a v^2 \tag{1b}$$

$$P_p = P_c p_p \eta_d \tag{1c}$$

$$P_p - (F_r + F_d)v = 0 \tag{1d}$$

In Figure 1 an overview of the forces acting on a system of bicycle and rider is given, where F_r is the rolling resistance, F_d the air resistance as defined in Equation 1, F_p the propulsion force, F_g the gravi-

Symbol	Description
F_r	Rolling resistance force (N)
c_r	Rolling resistance coefficient (-)
m_{tot}	Mass of rider and bicycle (kg)
g	Gravitational constant (m/s^2)
α	Slope (degrees)
F_d	Air resistance force (N)
A	Frontal are (m^2)
c_d	Drag force coefficient (-)
ρ	Air density (kg/m^3)
v	Speed [m/s]
P_p	Propulsion power (N)
P_c	Critical power (W)
p_p	Percentage of critical power taken (-)
η_d	Drivetrain efficiency (-)
d_b	Braking distance (m)
v_f	Final speed (m/s)
F_b	Braking force (N)
a_b	Braking deceleration (m/s^2)
F_g	Resistance force due to gravity (N)
ϕ_{max}	Maximum desired lean angle while coasting (degrees)
r_c	Radius of curvature (m)
$\phi_{pedalling}$	Maximum desired lean angle while pedalling (degrees)
v_d	Desired speed (m/s)
vi	Initial speed (m/s)
θ_s	Ratio of current speed over desired and initial speed (-)
$a_{cyclist}$	Acceleration of the cyclist (m/s^2)
a_m	Maximum acceleration (m/s^2)
v_c	Comfort speed (m/s)
ϵ	Uniform noise parameter (-)
P_r	Recovery power (W)
P_{rider}	Power provided by the cyclist (W)
F_{rider}	Force provided by the cyclist (N)
$F_{required}$	Total force require for desired acceleration (N)
P_w	Walking power (W)
m_{rider}	Mass of the rider (kg)
P_{met}	Metabolic equivalent power per kg bodyweight (W/kg)
m_{bike}	Mass of the bicycle (kg)
δ_h	Elevation difference (m)
t_{ahead}	Look ahead time (s)

Table 1: List of used symbols and units

tational force, α the angle of the slope and F_n the normal force.

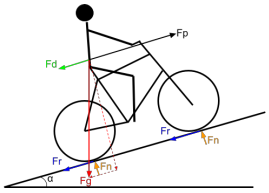

Figure 1: The forces acting on a bicycle and rider system on a slope

The propulsion power (P_p) in Equation 1 is defined by the critical power P_c, the human power percentage P_{pct} and the efficiency of the drivetrain η_d. The comfort speed is calculated by determining the speed the rider would reach on a flat straight road using his base power by solving Equation 1 for the speed v, where c_r is the rolling resistance coefficient, m_{tot} the combined mass of the rider and bicycle, Ac_d the combination of frontal area and air resistance coefficient and ρ the density of the air.

For e-bike users the comfort speed is calculated in the same way, thus without taking the power delivered by the e-bike motor into account. To compensate for the extra power the comfort speed is multiplied by 1.16, the average speed e-bike riders go faster than regular bicycle users in urban areas [7]. This driver power model makes the assumption that the rider is in optimal gear at all times, meaning that the gear is assumed to be at a optimal cadence to produce optimal power. The rider can therefore always deliver optimal power as gear changes are not part of this model.

The comfort speed is however not the speed the rider is always aiming for, the actual desired speed depends on the type of infrastructure the cyclist is riding on [8]–[12]. Four types of bicycle infrastructure are categorised: bicycle lanes, bicycle paths, shared roads and bicycle streets. Lanes are separated from car traffic by a (dashed) line, paths are completely separated from car traffic in a way that the bicycle path and car road will not have a common edge. Roads are defined as shared roads where both cars and bicycles can ride, usually found in residential areas. Lastly, bicycle streets are also shared with cars, the difference being that the cyclists have priority and cars have to ride at a slow pace. Because the highest speeds are attained on bicycle lanes [12], this infrastructure type is chosen as the standard where the comfort speed is calculated on, due to the comfort speed representing an unobstructed cyclist. For the other three infrastructure types a speed reduction is applied to the cyclist on top of his comfort speed, the reductions can be found in Table 2. From all found studies on bicycle speeds on infrastructure, only one was conducted in the Netherlands, it is assumed this study will give the most accurate values for Dutch cycling infrastructure.

Type	**Speed reduction [m/s]**
Lane	-
Path	0.463
Road	0.842
Street	0.049

Table 2: Bicycle infrastructure and speed reductions

2.1.2 Braking

Another reason besides infrastructure type for the desired speed to be lower is due to curves in the road, traffic lights or necessity to slow down to give way. These route characteristics can require the driver to stop pedalling or even brake when necessary. At the location of give way points a reduction in speed is used to make the cyclist slow down without stopping. The cyclists will want to reach a slower speed to overlook the traffic situation before starting to accelerate again. For traffic lights the desired speed is not set to zero, although the cyclists will come to a complete stop. This is because cyclist do not slow down to 0 km/h at traffic lights, but rather step off their bike while still carrying speed [13]. To include this behaviour in the model, the final speed a cyclist reaches at traffic lights by braking is set as a stop speed above zero with varying possible values per individual. No stop signs are present on the evaluated

routes, but they will lead to the same braking behaviour as traffic lights with the exception of a time the rider has to wait before starting to cycle again. In the model three types of braking are used: braking for stops, braking for curves, and braking when the speed exceeds the safety speed of the rider.

When braking for stops is required the initial and final speed are known. When cyclist brake for stops they use a constant deceleration, rather than a constant braking force [14]. From a predefined constant deceleration a_b and the current and requested final speed (v & v_f), the distance to the point ahead where a lower speed is desired can be calculated. This point ahead is the point at which the rider has to start braking (d_b), it is used to make the cyclist reach the desired speed at the point of interest, see Equation 2.

$$d_b = (v_f^2 - v^2)/2a_b \tag{2}$$

With a desired constant deceleration the required braking force can be calculated if all external forces are zero. However, the external forces are not zero and the braking force has to be adapted to compensate for this by subtracting all the external forces from the braking force calculation. These external forces are later added to the total force acting on the points mass to calculate the acceleration. This way the drag, rolling resistance and gravitational force have no impact on the deceleration and a constant deceleration is achieved. This is given in Equation 3, where F_b is the braking force and a_b the constant braking deceleration.

$$F_b = a_b * m_{tot} - (F_d + F_g + F_r) \tag{3}$$

For curves the braking behaviour is different, because curves are not a single point on the route, but a continuous obstacle the rider has to adapt to. During the ride the cyclist looks ahead a certain time to scout what lies ahead, this is a time rather than a distance to be applicable and salable to all speeds. The faster a cyclist goes through a curve, the more they have to lean into the curve to remain stable. This leaning in lateral direction relative to the direction of travel is defined by the lean angle. For all route points that would be reached in the look ahead time based on the current speed, the maximum of the curvatures ahead (r_c) and current speed (v) are used to calculate the lean angles that would be reached in the points ahead. This is done by Equation 4, which gives the relation between a constant speed and constant lean angle in a curve [15].

$$\phi_{max} = arctan(v^2/(gr_c)) \tag{4}$$

The lean angles ahead are compared to the maximum lean angle the rider wishes to achieve while pedalling ($\phi_{pedalling}$) and the maximum while coasting (ϕ_{max}), to detect when braking and coasting are required respectively. As soon as the lean angle ahead is above $\phi_{pedalling}$, the driver will start to coast, and when it reached above ϕ_{max} they will start to brake. The look ahead time and braking and coasting behaviour is modelled they way Nee and Herterich described, by having a coasting phase between the pedalling and braking phase [16]. The amount of braking force necessary is determined by the speed the rider wants to have in the curve (v_d which is calculated by Equation 5), the distance to the curve (d_c), the total mass of the rider and bicycle system (m_{tot}) and the speed at which the driver starts to brake (v_i), see Equation 6. This braking force leads to the driver reaching the required speed with a constant deceleration exactly at the point of curvature where the lean angle would be exceeded. In case the driver is already braking for a curve and sees a point ahead in time that would require him to break harder, for example when the curvature increases but braking is already needed before the maximum curvature is in sight, the required braking force is recalculated to make sure the maximum lean angle is never exceeded. An example of the braking force plotted over time together with the curvature is given in Appendix A.

$$v_d = \sqrt{tan(\phi_{pedalling})gc} \tag{5}$$

$$F_{braking} = (v_d^2 - v_i^2)/(2d_c)m_{tot} \tag{6}$$

The last type of braking behaviour is when the cyclist is going downhill without pedalling and the speed gets too high, exceeding the safety feeling of

the cyclist. When this maximum safety speed is exceeded the rider will brake to maintain the safety speed and to stop accelerating any further. In this case the required braking force is the sum of the other resistance forces: drag, rolling resistance and gravitational force. The downhill safety speed is estimated from previously used valued in literature to be 1.5 times the comfort speed [17], [18], above this the driver will start braking.

2.1.3 Acceleration

To reach the desired speed the cyclist will have to accelerate by providing more power than all resistances combined. Contrary to deceleration, the acceleration of a cyclist is not constant. The best representation of the natural acceleration of cyclists in a function is a two term sinusoidal function based on speed ratio [14] given in Equation 7, where θ_s is the ratio of speed over initial and final speed, v the current speed, v_i the initial speed and v_d the desired speed. The sinusoidal function is then made from the maximum acceleration (a_m) and constants ($C, B, c, a = \frac{-1}{1+c}$), see Equation 8.

$$\theta_s = \frac{v - v_i}{v_d - v_i} \tag{7}$$

$$a_{cyclist} = Ca_m(sin(\pi\theta_s)+Bsin(2\pi\theta_s))+\left(a + \frac{1}{\theta_s^2 + c}\right) \tag{8}$$

The maximum acceleration is estimated based on the comfort speed of the cyclist with Equation 9 [19], where v_c is the comfort speed. Because the linear relationship in the logarithmic space found by Ma and Luo only has an R^2 of 0.64 a layer of uniform noise in the range of [-0.5,0.5] ϵ is added to better capture the true spread in values.

$$log(a_m) = 0.8248log(v_c) - 1.3263 \tag{9a}$$

$$a_m = e^{(a_{ln})+\epsilon} \tag{9b}$$

For every combination of speed and desired speed the acceleration can be calculated and therefore the required power to be delivered by the rider to achieve that acceleration. A required power below the critical power can be maintained for many hours, therefore there are no limits on the power usage in that range in the model. When the required power is above P_c the rider will have to use anaerobic power, which is of limited supply. Anaerobic power is modelled as a energy storage that can either be drained to use extra power or refilled to regain energy over time. The maximum anaerobic force that the rider can provide is a constant percentage of the amount of energy that is left of the anaerobic work capacity (AWC). To simulate the rider never using full power, the same as with P_c, a percentage is taken of the anaerobic power to reduce the maximum available power. When the provided power by the cyclist is below P_c, the AWC will regenerate, although at a different rate than it is drained at. Equation 10 shows the recovery power (P_r) of the AWC, based on the provided power by the cyclist (P_{rider}) and P_c based on experimental data [20].

$$P_r = 0.08P_{rider} + 0.88P_c \tag{10}$$

2.2 E-bike power

When an e-bike is used, a part of the required power is delivered by the electric motor. In e-bikes there are two different kinds of motor control used in the Netherlands, cadence controlled and torque controlled. The first one only detects whether the cyclists is pedalling and provides a constant power based on the set assistance level, which is a percentage of the maximum motor power. In torque controlled e-bikes the motor measures the torque and cadence and therefore the power delivered by the cyclist to provide a percentage of that power. In both cases the motor assistance forces are only present at speeds up to 25 km/h due to European legislation, and have a maximum motor power of 250 W. It is possible that the power provided by cadence controlled e-bikes is already high enough to reach the required power, which leads to the rider not having to pedal and the motor not providing power as a consequence. To get out of this cycle the assistance level is lowered until at least a portion of the required power can be provided by the rider. Every time step the assis-

tance level is reset to the original value and lowered if needed to have the original assistance level active when possible.

For torque controlled e-bike motors the required force can be exactly split into a motor and a human part without altering the assistance level. The human part is given in Equation 11, where λ is the assistance level.

$$F_{rider} = \frac{F_{required}}{1 + \lambda} \tag{11}$$

2.3 Walking

On the route with a tunnel, the rider has to walk down stairs into the tunnel an walk back up the stairs to exit while guiding their bicycle. To include the energy usage of walking the stairs a metabolic equivalent is used, one for walking up and another for walking down. Both walking upstairs and downstairs require different amounts of energy. The energy usage is calculated based on the mass of the rider to account for the required energy to overcome the potential energy when walking upstairs. An average of multiple sources for metabolic equivalent is used with a value of 3.50 for downstairs and 8.73 for upstairs walking [21]–[23] with constant speed of 0.835 and 0.745 m/s [24] respectively. The metabolic equivalent describes the energy required to do a task per hour and dependent on the mass of the human. When walking upstairs the weight of the bicycle is included in the form of the difference in potential energy of the elevation difference, when going downstairs the impact of the bicycle is neglected. This results in the formula for walking power given in Equation 12, where P_w is the walking power in Watts, P_{met} the metabolic equivalent of task for either up or down, d is the direction of travel; 1 for up and 0 for down, and δ_h is the elevation difference in that time step.

$$P_w = 1.162 m_{rider} 0.2 P_{met} + d m_{bike} g \delta_h \tag{12}$$

A factor of 0.2 is taken as the human efficiency to make the energy used for walking equivalent to the energy that the human puts out instead of the energy representing the calories burnt, this is to make it the same as for the cycling part of the model.

3 Input data

3.1 Route data

The data for the routes is collected from different sources for different attributes of the route. There are also differences between data collection of the existing routes and the new bicycle highway route that is yet to be built. For the existing routes the latitude and longitude of route points are taken from Graphhopper [25], an online open source route planner. For the highway no route planner is possible, the route is modelled with the help of provided design drawing from the municipality of Den Haag. The elevation data from Graphhopper is not used, because elevation data from GNSS can be very inaccurate [5] and small differences in elevation can lead to large offsets in speed and therefore time. Because of this, a more accurate elevation data source is used in the form of LIDAR data. For the Netherlands there is open data available with classification [26]. This data is processed and smoothed, see Appendix B for the full explanation of the elevation data processing. An example of the elevation smoothed result is shown in Figure 2. The blue line shows the elevation obtained from the LIDAR data and the red line the fitted spline after filtering out overhead roads and other obstacles.

The coordinates in the horizontal plane are interpolated with a point every 10 m to increase the point density, as straights returned by route planners contain no intermediate points. Next, with the function *splprep* from the Python *Scipy.interpolate* package a B-spline is drawn through the points to get a smooth path with smooth curves, no smoothing factor is used in the spline to make sure the line goes through all points and the route does not diverge. Lastly the spline is interpolated to get a data point ever 0.1 m of the route, for each point the elevation is found with the LIDAR elevation map. To prevent sudden jumps in the elevation data, the data is smoothed by fitting a spline through the elevation data points.

Variable	μ	σ	Min	Max	Unit	Type	Source
m_{bike}	16.0	2.439	7.8	22.0	kg	field data	[27]
c_r	0.0077	0.0036	0.0012	0.0189	-	field data	[3]
c_dA	0.559	0.170	0.209	1.128	m^2	field data	[3]
p_p	0.655	0.0317	0.560	0.750	-	estimation from theoretical data	[6]
a_b	1.5	0.15	1	2	m/s^2	estimation from design guideline	[27]
ϕ_{max}	12.5	2.5	5	20	degrees	educated guess	[27], [28]
t_{ahead}	2	0.3	1	3	s	estimation from simulation data	[16]
η_d	-	-	0.86	0.97	-	experimental data	[29], [30]
Mass e-bike	-	-	6	8	kg	manufacturers data	[31]

Table 3: Input data distributions for rider and bicycle characteristics

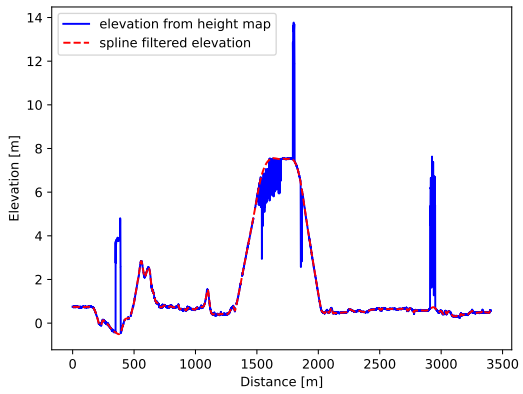

Figure 2: Elevation data obtained from the LIDAR height map and the fitted spline that filters the flyovers, tunnels and other obstacles.

Then for each data point a curvature is calculated based on the point itself and the 30 nearest points, 15 in front and 15 behind, to take the curvature over a total length of 3 m. Some points are close together in curves due to the route following the bicycle lanes and roads in a strict way. In reality cyclist will take wider turns making use of the available space. In combination with the fact the the interpolated route points make curves less smooth than the original line, because points are taken every 0.1 m, the extra curvature smoothing is applied to smooth out unrealistic sharp turns between data points that are very close together.

For the location of traffic lights online sources are available, but those are incomplete for bicycle routes. The locations of traffic lights are therefore based on Google Maps [32] satellite and street view images and later checked by physically riding the route. Locations where cyclists have to give way are determined in the same way. Give way points are modelled as a point where the rider has to slow down to look for crossing traffic, while coming to a complete stop is assumed to be unnecessary in most cases. For each point a random percentage (0-100%) of the cyclists comfort speed is taken that the cyclist has to slow down to. This way the cyclist reduces speed based on their comfort speed, so fast riders slow down to a relative higher speed than slower cyclists. In the case of traffic lights, real life data is made available by the municipality of Den Haag from which distributions of waiting times and green times can be calculated. This data is displayed in Appendix B. Only data from daytime is used, because both the wait time and green time are very different during night times due to the reduced amount of traffic. Utility cyclists are most active during day time, as traversing to work and shops is done then. Modelling the traffic lights and give way points with green light and slow down speed probabilities results in every cyclist having different behaviour around traffic lights and give way points.

3.2 Rider data

For the data about the cyclists, multiple sources and approaches are used. Most used parameters are assumed to be normal distributions with given mean and standard deviation, along with a maximum and minimum value to cut of the distribution at both ends to keep the data within realistic bounds. The exceptions are the variables where no normal distribution is found in literature and a uniform distribution is assumed between a minimum and maximum. In Table 3 the mean, standard deviation and bounds of each input variable are shown. The bike mass, rolling resistance, air resistance and drivetrain efficiency parameter values are based on measurement taken in other bicycle studies for utility cyclists. The human power percentage is estimated from training levels that represent low effort training, a limit around this range is taken. The braking deceleration is the value reported by the Dutch standards [27] for normal braking behaviour of utility cyclists, an estimation is made on the range of values. The maximum desired lean angle value is an estimation based on reported maximum speed per curve radius in the dutch design standards [27] and reported maximum wanted lean angle for regular cyclists [28]. The maximum lean angle while pedalling ($\phi_{pedalling}$) is taken as 70% of ϕ_{max} as no data source was found in literature that describes the lean angle at which a cyclists stops pedalling. The look ahead time is estimated from a cycling model [16] that implements look ahead time to make the rider slow down before hitting the curve. The range of values are similar to those of people walking on natural terrain [33] giving the idea that people look ahead the same time in both transport modes. The e-bike mass is the extra mass of an e-bike compared to regular bicycles, based on manufactures data.

The values for P_c and AWC are based on the sex of the cyclists, to implement this two different distributions are used, see Table 4. For the AWC values the bounds are set based on the maximum and minimum reported data [34], while for the mass and P_c parameters the bounds are set as: $\mu \pm 2\sigma$ to stay within realistic values and get close to the reported bounds on P_c. The bounds on the age are set to represent adults for which weight data is available.

Variable	Sex	Mean	Std	Min	Max	Unit
P_c	Male	204.77	37.76	129.25	280.29	W
	Female	152.25	23.58	105.09	199.41	
AWC	Male	16150	5460	4880	25550	J
	Female	8340	2200	3250	12680	
m_{rider}	Male	84.80	19.53	45.35	123.45	kg
	Female	72.50	19.53	33.45	111.55	
Age	Male	49.91	18.15	20	80	years
	Female	51.22	18.82	20	80	

Table 4: Input data sex dependent

When taking values from the input distributions to make a combination of cyclist and bicycle, correlations between parameters can be used to draw samples that represent more realistic combinations. For example, a cyclist with a high P_c and a very low weight will be unlikely as the low weight will indicate a lower muscle mass. To get more realistic combinations correlations where looked up in literature about utility cyclists. When no correlation is found the parameters are assumed independent, this is the case for most model parameters.

For four parameters correlations are found in literature: P_c, mass of the rider, age of the rider and the AWC [3], [35]–[38]. The correlation matrix is given in Table 5, which has a negative eigenvalues of -0.31 showing the matrix is not positive (semi-) definite which is a requirement for the matrix to be usable as a correlation matrix since a correlation matrix is positive (semi-) definite by definition [39]. This problem is solved by finding the closest matrix that is positive (semi-) definite [39], this will change the correlations without changing the standard deviations of the variables. The real standard deviations are then used to create a usable covariance matrix. All four of these correlated parameters are also dependent on the sex of the cyclist, which is either male or female. When the sex of the rider is determined the mean and standard deviation of the age of the cyclist is set based on the population data of the Netherlands [40] with a lower limit of 20 and upper limit of 80 years. In similar way the mass distributions are made, with bounds defined as the mean plus and minus two times the standard deviation [41]. Lastly the AWC values are also set based on the sex, followed by the P_c. For

	CP	AWC	Age	Mass rider
CP	1	-0.546	0.377	0.745
AWC	-0.546	1	-0.477	0.645
Age	0.377	-0.477	1	0.15
Mass rider	0.745	0.645	0.15	1

Table 5: Correlation matrix

both male and females a different distribution of age, mass, AWC and P_c is used that results in two different covariance matrices build from the same correlation matrix. With all means and standard deviations defined a correlated sample can be drawn.

The third category of input variables are those linked to the e-bike, based on Dutch demographic data [4] the share of owning an e-bike per age are used to randomly assign an e-bike to the simulated cyclist. In addition, the type of e-bike is randomly picked between torque and cadence controlled with equal weight. Lastly, the assistance level is chosen at random, for torque controlled this is between 0 and 2.5 and for cadence controlled between 0 and 1, with increments of 0.5 and 0.2 respectively.

4 Case study

4.1 Route descriptions

A case study in the Dutch city of Den Haag is used to show the utility of the model. In Den Haag a new part of a bicycle highway is planned for construction between the train stations Holland Spoor (A) and Laan van Noi (B). Six routes are evaluated and compared, the first one is the fastest current cycling route between the two stations, which will be referred to as flyover due to the route making use of a flyover to the north to cross the train track perpendicular to the route. The flyover makes the cyclists climb, increasing the required energy compared to a flat route. A part of this energy is recovered by going down the slope again, but the presence of traffic lights and give way points after the descend results in the cyclists having to brake and losing the regained energy again. This route is the longest as ist makes a detour to be able to cross the train tracks. The second route, the tunnel route, makes use of a tunnel under the train tracks instead of the flyover. Cyclists have to walk down and up stairs with their bicycle to enter and exit the tunnel, while cycling is allowed in the tunnel. This tunnel shortens the distance and removes the climb on the flyover, but introduces stairs where the cyclists is slowed down due to having to brake for the stairs and walking them up and down with their bicycle in hand. The amount of traffic lights is lower compared to the flyover route, although the difference is small. The third and last route is a new planned bicycle highway which takes a more direct path parallel to the train tracks between the two train stations, this route is called called highway. From the three routes the highway is the most direct, resulting in the lowest distance. The amount of traffic lights is brought to a minimum by avoiding crossings as much as possible. To cross the train tracks this route uses an elevated road with relatively short ramps, meaning that the cyclists have to overcome a steep hill. Moreover all routes are evaluated in both directions, east and west, due to differences in road elements such as traffic lights as well as differences in route layout. Only for the highway route the layout in both directions follows the same road, being on the opposite side. An overview of all routes is given in Figure 3.

4.2 Simulation parameters

The system of equations is solved for speed and time using using the function $solve_ivp$ from the *scipy* library in Python. The 5th order Runge-Kutta method is used to solve the differential equation that results from the sum of all forces, default values of 1e-3 for the relative tolerance and 1e-6 for the absolute tolerance are used.

4.3 Number of simulations

For all six routes a standard error of the mean of 1% for the travel time is used as desired accuracy, with a used confidence of 95%. Per route 400 simulations were conducted after which the desired value was reached for every route. A standard error of the mean of 1% means that the final mean of the output

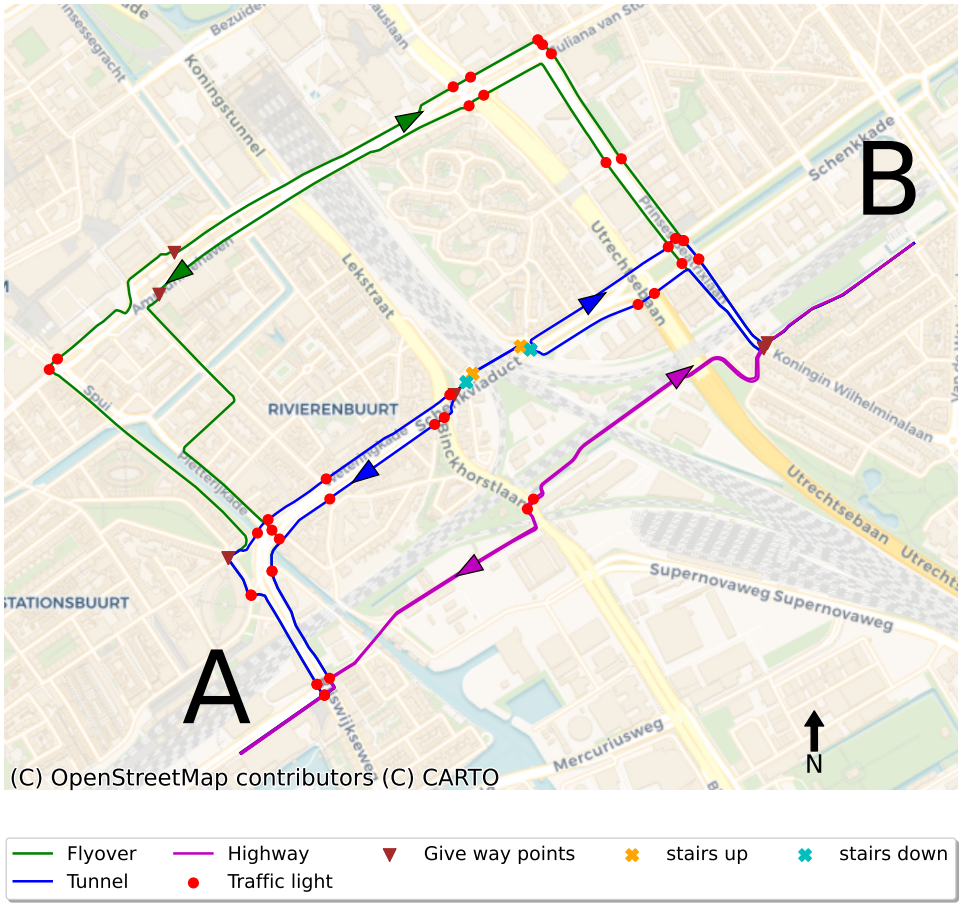

Figure 3: The six routes in Den Haag with the direction of travel indicated with an arrow. The crossings with the train tracks are shown, for the flyover and highway route the path goes over the railway. The tunnel routes goes under the railway with a tunnel.

will be within a range of 1% of the estimated real mean. Because the true mean is unknown, the estimated mean is used to calculate the required amount of runs with Equation 13, where n is the number of runs required, z the z value of 1.96 for 95% certainty, e the standard error of the estimated mean and s the standard deviation of the output data [42].

$$n = ((zs)/e)^2 \tag{13}$$

5 Results

To get a general overview of the output for different routes the mean travel time and energy expenditure can be compared. The standard deviation in the results can give an indication of the complexity of the routes, a simpler route with relatively fewer obstacles such as traffic lights and sharp curves could give a smaller spread in values. This could mean that not everyone profits the same from better routes, a narrower distribution would mean that slower cyclist

gain more time on the bicycle highway than faster cyclists. Moreover, a more coherent groups of cyclist may have a higher average speed than a group with a large spread in speeds, possible increasing the average speed of all cyclists. In Table 6 the means and standard deviations are given. In both directions the standard deviation of both the time and energy of the bicycle highway are lower than the ones for the tunnel routes, which are in turn lower than the flyover routes. This indicates that a shorter and/or simpler route will reduce the spread in both time and energy values.

Direction	**Route**	**Travel time**		**Energy**	
		μ [s]	σ [s]	μ [kJ]	σ [kJ]
East	Flyover	832.12	75.50	74.49	22.80
	Tunnel	608.67	52.99	54.90	15.41
	Highway	417.01	41.83	42.09	11.88
West	Flyover	910.97	81.66	82.06	24.50
	Tunnel	734.45	62.98	59.78	18.62
	Highway	404.15	39.94	44.10	13.29

Table 6: Mean and standard deviation of travel time and energy expenditure

Direction	**Route**	**Time**	**Energy**
East	Flyover	.269	.132
	Tunnel	.614	.507
	Highway	.072	.446
West	Flyover	.289	.099
	Tunnel	.714	.600
	Highway	.096	.170

Table 7: P-values of fitted Gaussian and skewed Gaussian for the energy and time distributions respectively per route
* $p < .05$
** $p < .01$
*** $p < .001$

On all combinations of the six routes for both time and energy a Kruskal-Wallis test is performed. Every combination results in p<.000, except for the comparison of the highway east with highway west, which gives p=.010. Therefore, all are significant on a level of 95 %, while all but the highway comparison are significant on the 99.9 % level showing that all routes are different in time and energy outcomes and that using the routes in two different directions gives different results.

With the time and energy distribution for each route the probability that one route is faster or requires more energy than another route can be calculated. Instead of comparing the means of the routes, comparing the full distribution can show if certain routes are better suited for a certain type of cyclist and give a measure of how much better a route is in factors of time and energy expenditure. First the shape of the output distributions is examined in Figure 4, where the distribution for time and energy output of the flyover route in east direction can be found together with the estimated Gaussian distributions based on the output's mean and standard deviation. While the time output shows a distribution closely resembling the Gaussian, the energy output shows a larger spread of data points and is therefore approximated by a skewed normal distribution. With a Kolmogorov-Smirnov test the fit of the (skewed-) Gaussian can be evaluated. The null hypothesis is that the distribution is the same as the reference for all data points, meaning that a higher p-value will show a better approximation of the reference distribution. The resulting p-values are given in Table 7, where it can be seen that up to a significance level of 99.9 % the null hypothesis can not be rejected and the approximations for the Gaussian and skewed Gaussian for the time and energy distributions respectively are significantly good approximations. For the time the probability of the travel time for one route A being lower than the values of another route B can directly be calculated by subtracting the means and forming a new distributions from the two normal distributions and finding the probability that the Z of the new distribution is above zero, as described in Equation 14.

$$P(A > B) = P(A - B > 0) = P(Z > 0) \qquad (14)$$

For the comparison on energy values the same calculation is not directly possible due to skewed normal distributions being used. Therefore the probability is

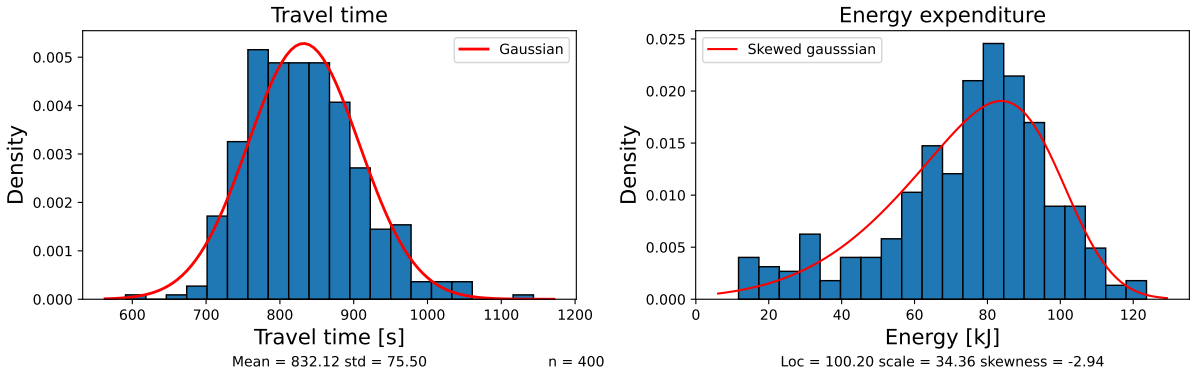

Figure 4: Results in energy and time expenditure for the whole population of the flyover east route, with fitted Gaussian and skewed Gaussian for the time and energy distribution respectively

calculated by drawing one million samples from both distributions and counting the mean amount of times the energy value from distribution A is higher than B. The probabilities of one route being faster than another or requiring more energy are shown in Table 8.

Direction	Route A	Route B	$\mathbf{P}(A_t > B_t)$	$\mathbf{P}(A_e > B_e)$
East	Flyover	Tunnel	0.992	0.773
	Tunnel	Highway	0.998	0.752
	Flyover	Highway	1.000	0.890
West	Flyover	Tunnel	0.956	0.774
	Tunnel	Highway	1.000	0.762
	Flyover	Highway	1.000	0.907

Table 8: Comparison of time and energy requirement in different routes

The probability in terms of time is either one or close to one in all cases meaning that the bicycle highway is almost always faster than the tunnel route, which is in turn almost always faster than the normal route. When comparing the energy requirement the outcome is less unanimous, there is a probability around 75 % that the flyover route requires more energy than the tunnel route or the tunnel route requires more than the highway route. For the comparison between the flyover and highway route the difference is smaller with a probability of 90% that the first has a higher energy requirement. A possible explanation for this is that e-bikes have a large impact on the energy while having a relatively small impact on the travel time. When only regular bikes are compared, see Table 9, the probabilities for energy requirement are higher but still not as close to one as the values for travel time showing that there are more factors at play than only e-bikes. Other possible factors are the amount of elevation in a route and the amount of necessary slow downs for either traffic lights or sharp curves, the characteristics of all routes are given in Appendix C.When looking at e-bikes only, the time probabilities are once again close to 1, while the energy probabilities average to 54 % indicating that for e-bike users the difference in energy between two routes is of no importance as neither route requires more energy than the other. These results of e-bikes are based on the modelled behaviour of assistance level choice and will therefore not fully represent real human behaviour.

Direction	Route A	Route B	$\mathbf{P}(A_t > B_t)$	$\mathbf{P}(A_e > B_e)$
East	Flyover	Tunnel	0.995	0.918
	Tunnel	Highway	0.999	0.882
	Flyover	Highway	1.000	0.990
West	Flyover	Tunnel	0.971	0.899
	Tunnel	Highway	1.000	0.881
	Flyover	Highway	1.000	0.997

Table 9: Comparison of time and energy requirement in different routes for regular bikes

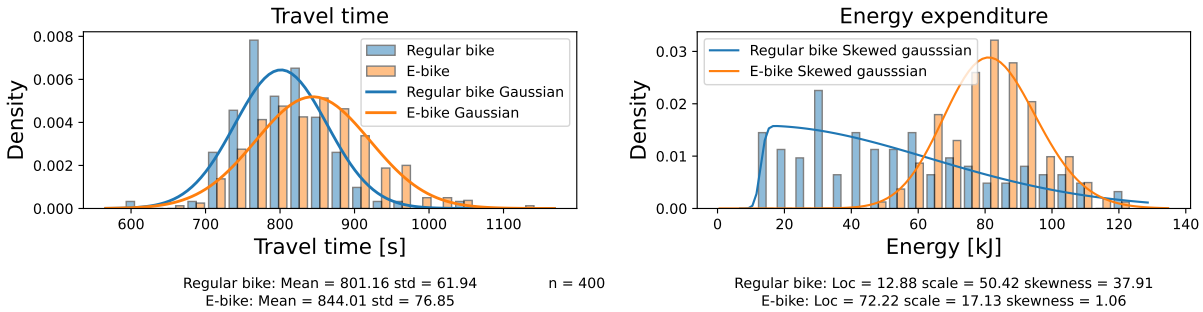

Figure 5: Results of the flyover east route split between e-bike and regular bike users

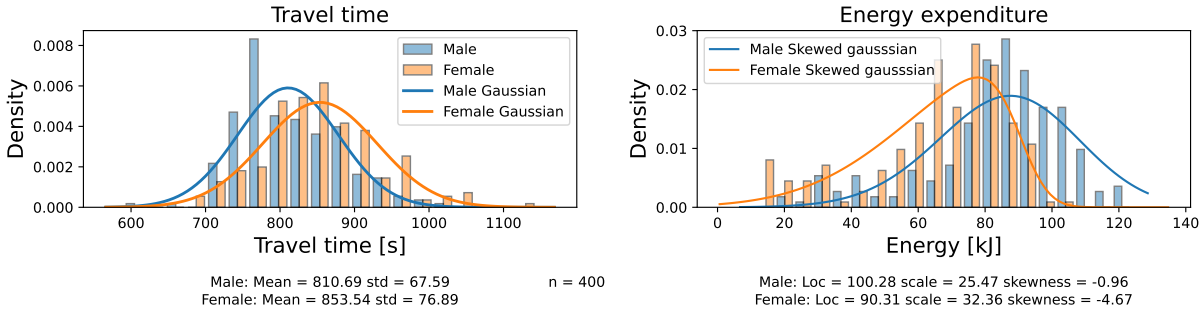

Figure 6: Results of the flyover east route split between male and female riders

The larger spread in energy usage compared to the time distribution can be explained when the data is split into e-bike an regular bike users, see Figure 5, where the regular bike users show a more as expected normal like distribution with a skewness close to one and the e-bike users a more flattened and less normal like distribution. Note that the energy in the figure is the human component of the energy, the energy provided by the e-bike motor is not included. Due to the e-bike users energy expenditure heavily depending on the chosen assist level, which is randomly picked and uniformly distributed, the energy output is more in line with a combination of the expected normal distribution similar to regular bicycles and the uniform distribution of the assist level. When the output is split into a regular and an e-bike category it becomes visible how much less energy e-bike users consume in comparison. The difference between the two groups is evaluated with a Kruskal-Wallis test, with null hypothesis that the population means are equal. This test results in a p-value of $<.000$, showing that the null hypothesis can be rejected up to a significance level of 99.9 %, see Table 10. These results might give an indication that although e-bikes can lead to faster travel times, the energy usage of riders is drastically lower leading to the major reason to get more people to use the bicycle, namely fitness and health benefits, becoming less present when comparing the same route for regular bicycles and e-bikes. The way e-bikes are modelled in this research the average energy usage is more than five times lower than that of regular bicycle users. However, the amount of energy used is highly dependant on the chosen assist level, therefore no accurate comparison between energy usage on regular and e-bikes can be made.

The data can also be split between male and female

		Time	Energy
Sex	**Male** **Female**	<.000***	<.000***
Age	**20-40** **40-60** **60-80**	.366	.323
Bicycle type	**E-bike** **Regular**	<.000***	<.000***
E-bike control	**Torque** **Cadence**	.430	.185

Table 10: Kruskal-Wallis test results for the flyover route east
* $p < .05$
** $p < .01$
*** $p < .001$

cyclists, as can be seen in Figure 6. Noticeable differences are the significant lower mean travel time and higher mean energy expenditure for males, although both distributions show a similar shape. This difference in time and energy is as expected as there are different inputs for either male or female for the distributions for both P_c and AWC, although males do have a higher mean mass, which will slow them down relatively to females. The extra power greatly outweighs the higher mass, a higher base energy output therefore clearly results in more energy usages and lower travel times. It might be possible that people with a higher mean power will tend to use a lower percentage of their power in reality. With more reliable power output percentage data more accurate conclusions can be drawn from male and female distributions. The distributions with time and energy for all routes can be found in Appendix D, all with similar results.

If the data is split between the two types of e-bike control in Figure 7, no significant differences in either travel time nor energy expenditure are observed, see Table 10. The main difference between the control types impacting time is the delivery of power when accelerating from standstill, which has a small impact on the overall behaviour of the model. Due to relatively low power demands on the evaluated routes, cadence controlled e-bikes can provide all power even at sub maximum assistance levels. Because of this the power provided by the cyclists can become extremely low leading to low energy expenditures. For torque controlled e-bikes the power provided by the motor is a percentage of the input power of the human rider and will therefore not drastically reduce the human energy expenditure on relatively low power demanding routes. When the control types are modelled in a more detailed way concerning power and torque delivery the differences between the two types may change. For now no significant distinction can be made between the two control types.

Lastly the time and energy distributions can be split between different age groups, see Figure 8. In this comparison the differences in time are small and not significant. A post hoc evaluation is done with the Kruskal-Wallis test, to compensate for the comparison of three groups in the data an adjustment method in the form of Holm's method is used, see Table 11. Due to a positive correlation between age and P_c older riders are expected to have higher energy outputs and therefore faster travel times. This correlation is made from test data on fit young participants and will therefore not give an accurate view when extrapolated to people outside the scope such as older people. The increase in P_c is compensated by the negative correlation of age with AWC and a positive one for rider mass. On top of this the chance of owning an e-bike is much higher for older people. When looking at the results all distributions of time and energy are close together, but people between 60 and 80 are on average a bit faster. No significant differences are found between cyclists of different ages, indicating that age does not play a large part in the travel time and energy expenditure of a population of cyclists.

Another possible angle is to look at the impact of traffic lights in a route, in Figure 9 the results of the flyover in east direction are given. The data is split between the amount of green traffic lights where the total amount of traffic lights on the route is nine. There are no simulations where there are 8 or 9 green lights for the cyclists. The mean travel time and energy expenditure for each group of an amount of green lights are compared to the mean time and energy of the whole population on the flyover east

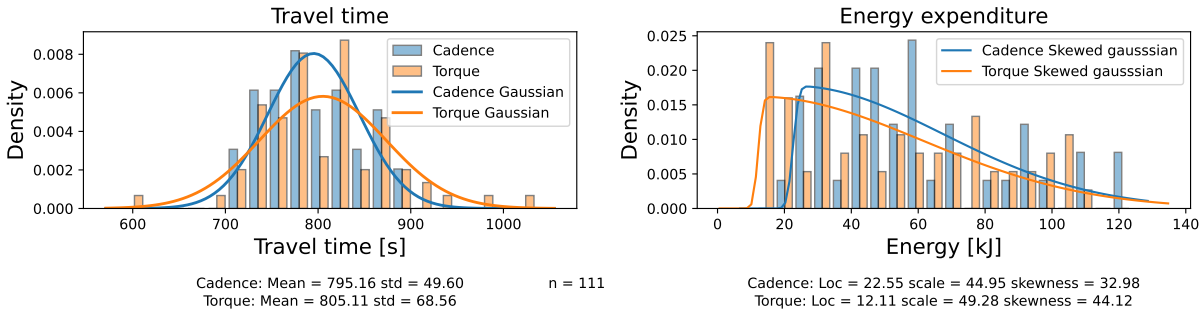

Figure 7: Results of the flyover east route split between torque and cadence controlled e-bikes.

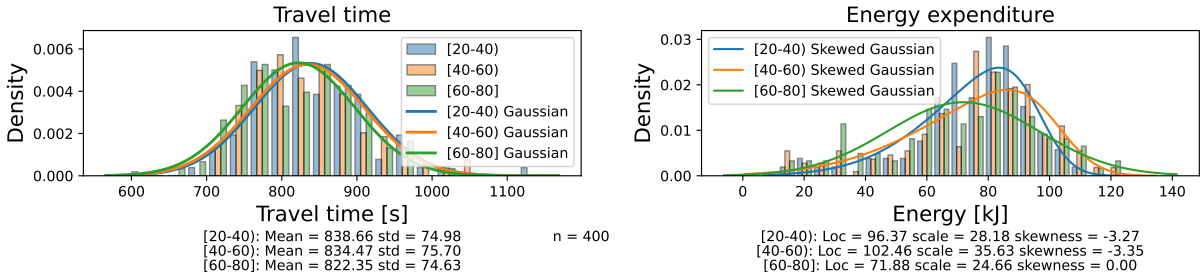

Figure 8: Results of the flyover east route split into 3 age groups.

		[20-40)	[40-60)	[60-80]
Time	**[20-40)**	-	.635	.529
	[40-60)	.635	-	.548
	[60-80]	.529	.548	-
Energy	**[20-40)**	-	.862	.862
	[40-60)	.862	-	.398
	[60-80]	.862	.398	-

Table 11: Dunn's test results for the flyover route east for different age groups with Holm's adjustment method
* $p < .05$
** $p < .01$
*** $p < .001$

route. It can be seen that the mean travel time will not always decrease with more green lights, and the required energy can even increase. Apart from the amount of green traffic lights, it is also important which lights are green. A stop right after a downhill section will require the cyclist to brake more and therefore lose more energy and time compared to a traffic light on a flat road or just after a sharp curve. The amount of data points is low for the extreme cases, zero green lights occurs eight times while seven green lights occurs only once. To get a better view at the impact of traffic lights on a route more simulations are needed to obtain sufficient numbers. The energy requirement fluctuates and goes both up and down for more green lights. This can be explained by the limited sample size, where one group has cyclists that have a higher power output than another group while having less green lights. An alternative to increasing the sample size is using the same cyclists and bicycles combinations for different amount of traffic lights to limit the variability. An overview of the traffic light data for other routes is given in Appendix E.

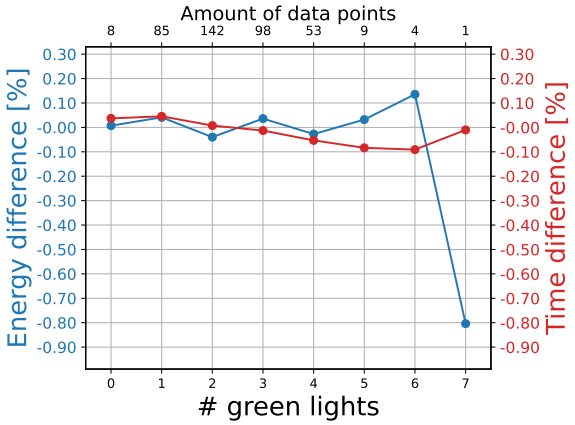

Figure 9: Energy and time reductions for number of green lights relative to the route mean

6 Discussion

6.1 Discussion of results

With the model presented in this research bicycle routes can be compared in matters of energy and time expenditure, which can lead to new insights. It has become evident that rider and bicycle characteristics can have a large impact on travel time and energy expenditure, although not all parameters lead to significant differences. The model can give an overview if a routes benefits certain cyclist types and even more important: how much it benefits them. By being able to quantify travel time and energy expenditure differences, route comparisons can be evaluated at a higher level. When a new route is planned, alternative designs can be compared to see how much it would benefit the expected type of users. This can also be adapted to different demographics, cities with a large share of e-bikes might not want the same bicycle infrastructure as cities with a low share of e-bikes. The same can be said for other demographic differences such as age or sex. In combination with studies about cyclist route choice the model can simulate routes and find if a route design is attractive for cyclists, or if alternative routes will lead to more people choosing the bicycle as type of transport.

The biggest shortcoming of the current model is the realistic modelling of human behaviour. There is little known about the power utility cyclists choose to ride with or when they decide to start coasting and braking. This behaviour aspects can have a large impact on the results and should therefore be modelled as close to reality as possible.

From the analyzed routes in the case study is has become clear that bicycle routes have to be evaluated in both directions, because even if the route follows the same road in both directions, the infrastructure elements such as traffic lights can still differ. The case study also shows that large elevation gains in bicycle routes will have a large impact on both the time and energy expenditure of utility cyclists, although a note has to be made that the routes that where compared where not of the same length. Another observation is that simpler routes, shorter and with less route elements, will lead to a more uniform flow of cyclists as the standard deviation in travel time reduces.

6.2 Sensitivity analysis

The model has many input variables, the accuracy of the used values can be very important to get accurate results. To find out which parameters have to most impact on the travel time and energy expenditure, and therefore need the most attention when defining values, a sensitivity analysis is performed on the tunnel west route. To be able to make comparisons between two simulations the traffic light and give way point behaviour has to be kept constant, therefore all traffic lights are modelled to be red and have waiting times of two seconds. All give way points have the rider reduce speed by 50 %. A baseline simulation is done, together with a simulation for every parameter with an increase of 5 % which is compared to the baseline. An increase of 5 % in rider mass results in a 2.22 % increase in energy usage, showing that mass together with elevation plays a large roll in energy requirements. Other parameters that have large impact are the drivetrain efficiency and the percentage of maximum human power used with energy requirements being -2.41 and 1.99 % respectively. The human power percentage leads to a almost 2 % increase in energy, while the time gain is only 0.9 %.

More power input will not give the same percentage of time gain as air resistance does not scale linear with speed. When e-bike motors are turned on in the model the time gain for both control types is 4.33 % with assist levels of both 0.6 and 0.8. This is due to the limitation of e-bikes that the motor can only apply power when the speed is not over 25 km/h. The energy requirements for these e-bike simulations are all as expected lower than the baseline, ranging from 25 to 68 % lower energy requirement. A full table of the sensitivity analysis results is given in Appendix F.

6.3 Simulation limitations of the model

In order to have enough time to perform all simulations the tolerances in the solver were not strict enough to make the cyclist stop at the desired speed at traffic lights. This results in overshooting the speed at which a rider arrives at a traffic light, a more detailed explanation is given in Appendix G.

A second limitation is the absence of an in field validation of the model. The outputs for travel time and energy expenditure are within realistic bounds, this is checked by calculating the time for the route distance with mean cycling speeds and using that time with average power. However, a validation with in field measurements is not present. A comparison with real life data could first of all give an indication of the true travel time and energy expenditure with a realistic power profile. The power profile will most likely have a high variability due to human behaviour, but general aspects such as places where extra power is provided can be better identified and validated.

6.4 Future applications

There are many possible use cases thinkable for the cycling model described in this research, one example is the impact of traffic lights. By taking out or adding traffic lights the impact on time and energy usage can be calculate for a population of cyclists leading to new insights for city planners. This can be extended to making green waves, in which cyclist will have a green light multiple times in a row by making the lights go green based on the time it will take a cyclists to go from one traffic light to the next. For a population of cyclist it can be found how much time is needed in between lights, as well as the required duration of the green time. Other possible applications include the possibility to help city planners quantify differences between planned routes and existing infrastructure.

6.5 Recommendations

In this paper the most important features for an energy and time cycling model are implemented, a feature that is often named but not used is wind. Wind can have a large effect on the cyclists based on both the wind speed and direction, but is highly unpredictable especially in urban areas with high buildings. Possible implementations are either using a constant wind speed or a distribution of possible region specific speeds and directions. While on average the wind might equal out as the route is traversed in both directions, it is possible that cyclist prefer to take another route based on wind speed and direction.

Another possible addition to the model is the way traffic lights are implemented, there is no dynamic behaviour of the cyclist as the color of the light is predetermined. In reality a cyclist may give extra power to make a yellow or green light or make a hard stop if the light suddenly changes to red. Using this dynamic behaviour in the model would require the rider to make a choice leading to a new layer of possibilities lying outside the scope of this research. In addition, implementing red light running could lead to more realistic behaviour, especially at traffic lights where cyclists often do not stop for red lights.

Regarding the used features, some variables are not well documented in literature such as the look ahead time, maximum desired lean angle and the percentage of human power. These are often described in models that minimize time and maximize power, which is not applicable to utility cycling. The same is true for constants used in the AWC deployment and regeneration. Moreover, power values are taken from experiments that are conducted on mostly fit young people, while little is known about older and less fit people. The maximum desired lean angle is estimated on a flat road, while in reality cyclists may desire a

lower angle for downhill curves due to reduced grip. For all of these inputs further research is needed to get realistic values for utility cyclist.

7 Conclusion

The goal of this research was to develop a bicycle model that simulates utility cyclists on a route and gives distributions of travel time and energy expenditure for a population of cyclists. This model can be a new way to compare different bicycle routes in the planning phase with both alternative plans and existing routes based on a population of different kind cyclists and bicycles. A case study was performed where the differences in time and energy expenditure for a population of cyclists on three different routes all in two direcrtions were evaluated. The first route makes a detour to cross a train track and makes use of a flyover to cross it. The second route is shorter and uses a tunnel to cross the tracks, the tunnel is accessible by stairs that the cyclists has to traverse. The third route is a newly planned bicycle highway that crosses the train tracks with a new bridge, making this route the shortest and most direct. A Monte Carlo simulation was conducted with ranges of input parameters about the rider and bicycle characteristics as well as dynamic route characteristics in the form of traffic lights. A significant gain in time is found for almost the whole populations for the highway route over the tunnel route and for the tunnel route over the flyover route showing that the routes results in significant differences in travel time. Next to the time gain the energy requirement follows the same trend, with the key difference that the energy requirement has a lower probability of being lower in said route comparisons. This is mostly due to the use of e-bikes, for them there is close to no difference in energy requirement between routes. Future model extensions could implement wind as most important new factor, while better input data is needed to obtain more accurate results.

References

[1] I. N. Sener, N. Eluru, and C. R. Bhat, "An analysis of bicycle route choice preferences in texas, us," *Transportation*, vol. 36, pp. 511–539, 5 Apr. 2009, ISSN: 00494488. DOI: 10.1007/S11116-009-9201-4/TABLES/4.

[2] B. v. W. Eva Heinen and K. Maat, "Commuting by bicycle: An overview of the literature," *Transport Reviews*, vol. 30, no. 1, pp. 59–96, 2010. DOI: 10.1080/01441640903187001.

[3] A. Bigazzi and R. Lindsey, "A utility-based bicycle speed choice model with time and energy factors," *Transportation*, vol. 46, pp. 995–1009, 3 2019, ISSN: 00494488 (ISSN). DOI: 10.1007/s11116-018-9907-2.

[4] RIVM, *Elektrische fietsen in nederland*, https://www.rivm.nl/documenten/factsheet-elektrisch-fietsen-in-nederland, (Accessed on 12/5/2024).

[5] M. Rothhämel, "A detailed bicycle energy model and its application in infrastructure assessment," *SSRN Electronic Journal*, Apr. 2022. DOI: 10.2139/SSRN.4088432.

[6] A. C. C. Howe. "The road cyclist's guide to training by power part i: An introduction." (2007), [Online]. Available: https://jpansy.at/wp-content/uploads/2011/03/racing-by-power.pdf.

[7] S. I. for Road Safety Research, *Elektrische fietsen en speed-pedelecs*, https://swov.nl/sites/default/files/bestanden/downloads/FS%20Elektrische%20fietsen_1.pdf, May 2022.

[8] S. Bernardi and F. Rupi, "An analysis of bicycle travel speed and disturbances on off-street and on-street facilities," *Transportation Research Procedia*, vol. 5, pp. 82–94, Jan. 2015, ISSN: 2352-1465. DOI: 10.1016/J.TRPRO.2015.01.004.

[9] A. El-geneidy, K. J. Krizek, and M. J. Iacono, "Predicting bicycle travel speeds along different facilities using gps data: A proof-of-concept model," in *Proceedings of the 86th Annual Meeting of the Transportation Research Board*, 2007.

[10] A. Knight and S. G. Charlton, "Protected and unprotected cycle lanes' effects on cyclists' behaviour," *Accident Analysis & Prevention*, vol. 171, p. 106 668, Jun. 2022, ISSN: 0001-4575. DOI: 10.1016/J.AAP.2022.106668.

[11] A. Clarry, A. F. Imani, and E. J. Miller, "Where we ride faster? examining cycling speed using smartphone gps data," *Sustainable Cities and Society*, vol. 49, p. 101 594, Aug. 2019, ISSN: 2210-6707. DOI: 10.1016/J.SCS.2019.101594.

[12] H. Yan, K. Maat, and B. van Wee, "Cycling speed variation: A multilevel model of characteristics of cyclists, trips and route tracking points," *Transportation*, pp. 1–30, Apr. 2024, ISSN: 15729435. DOI: 10.1007/S11116-024-10477-6/TABLES/4.

[13] M. Hogetoorn, "Dense cycling conditions," Master's Thesis, Delft University of Technology, 2022. [Online]. Available: https://www.victorknoop.eu/research/theses/2022_hogetoorn.pdf.

[14] H. Twaddle and G. Grigoropoulos, "Modeling the speed, acceleration, and deceleration of bicyclists for microscopic traffic simulation," *Transportation Research Record*, vol. 2587, pp. 8–16, 1 2016, ISSN: 03611981 (ISSN). DOI: 10.3141/2587-02.

[15] D. Karnopp, *Vehicle Dynamics, Stability, and Control*. CRC Press, Apr. 2016, ISBN: 9780429096822. DOI: 10.1201/b13767.

[16] P. J. Nee and J. G. Herterich, "Modelling road cycling as motion on a curve," *Sports Engineering*, vol. 25, pp. 1–14, 1 Dec. 2022, ISSN: 14602687. DOI: 10.1007/S12283-022-00376-3/FIGURES/8.

[17] R. Goussault, A. Chasse, and F. Lippens, "Model based cyclist energy prediction," vol. 2018-March, Institute of Electrical and Electronics Engineers Inc., 2018, pp. 1–6, ISBN: 978-153861525-6 (ISBN). DOI: 10.1109/ITSC.2017.8317645.

[18] D. Grossoleil and D. Meizel, "Modelling the hybridisation of human and artificial energy applied at an electrical bicycle," vol. 11, IFAC Secretariat, 2010, ISBN: 14746670 (ISSN); 978-390266194-4 (ISBN). DOI: 10.3182/20100831-4-fr-2021.00073.

[19] X. Ma and D. Luo, "Modeling cyclist acceleration process for bicycle traffic simulation using naturalistic data," *Transportation Research Part F: Traffic Psychology and Behaviour*, vol. 40, pp. 130–144, 2016, ISSN: 13698478 (ISSN). DOI: 10.1016/j.trf.2016.04.009.

[20] F. Ashtiani, V. S. Sreedhara, A. Vahidi, R. Hutchison, and G. Mocko, "Experimental modeling of cyclists fatigue and recovery dynamics enabling optimal pacing in a time trial," Jul. 2019. DOI: 10.23919/ACC.2019.8814854.

[21] K. C. Teh and A. R. Aziz, "Heart rate, oxygen uptake, and energy cost of ascending and descending the stairs.," *Medicine and science in sports and exercise*, vol. 34, no. 4, pp. 695–9, Apr. 2002.

[22] D. R. Bassett, J. A. Vachon, A. O. Kirkland, E. T. Howley, G. E. Duncan, and K. R. Johnson, "Energy cost of stair climbing and descending on the college alumnus questionnaire," eng, *Medicine and science in sports and exercise*, vol. 29, no. 9, pp. 1250–1254, 1997, ISSN: 0195-9131. DOI: 10.1097/00005768-199709000-00019.

[23] B. E. Ainsworth, W. L. Haskell, M. C. Whitt, *et al.*, "Compendium of physical activities: An update of activity codes and met intensities," *Medicine and science in sports and exercise*, vol. 32, no. 9, 2000.

[24] T. Fujiyama and N. Tyler, "An explicit study on walking speeds of pedestrians on stairs," *10th International Conference on Mobility and Transport for Elderly and Disabled People*, May 2004.

[25] *Graphhopper*, https://www.graphhopper.com/, 2024.

[26] GeoTiles, *Geotiles: Readymade geodata with a focus on the netherlands*, https://geotiles.citg.tudelft.nl/.

[27] CROW, *Crow kennisbank*, https://kennisbank.crow.nl/, (Accessed on 02/04/2024).

[28] H. Abdelsalam, M. Borhan, A. Milad, H. Imhimmed, and R. Rahmat, "Developing a web-based advisor expert system for green transportation system," *Journal of Theoretical and Applied Information Technology*, vol. 1595, p. 9, Jul. 2017.

[29] B. Rohloff and P. Greb, "Efficiency measurements of bicycle transmissions-a neverending story ?" In *Technical Journal of the IHPVA*, 2004.

[30] C. Kyle and F. Berto, "The mechanical efficiency of bicycle derailleur and hub-gear transmissions technical notes," *Technical journal of the IHPVA*, pp. 3–11, 52 2001.

[31] Gazelle, *Knowledge base ebikes*, https://www.gazellebikes.com/en-us/knowledge-base/electric-bikes/weight, (Accessed on 05/02/2024).

[32] G. Maps, *Den haag*, https://www.google.nl/maps, (Accessed on 15/07/2024).

[33] J. S. Matthis, J. L. Yates, and M. M. Hayhoe, "Gaze and the control of foot placement when walking in natural terrain," *Current Biology*, vol. 28, 1224–1233.e5, 8 Apr. 2018, ISSN: 09609822. DOI: 10.1016/J.CUB.2018.03.008.

[34] J. M. Eckerson, J. R. Stout, G. A. Moore, *et al.*, *Effect of creatine phosphate supplementation on anaerobic working capacity and body weight after two and six days of loading in men and women*, 2005.

[35] M. A. Kantor, J. Albers, K. Weed, and Z. O. Erickson, "Critical power concept: Males vs. females and the impact of muscle fiber composition," *International Journal of Exercise Science*, vol. 12, pp. 277–286, 4 2019.

[36] G. Bourgois, P. Mucci, J. Boone, *et al.*, "Critical power, w and w reconstitution in women and men," *European Journal of Applied Physiology*, vol. 123, pp. 2791–2801, 12 Dec. 2023, ISSN: 14396327. DOI: 10.1007/S00421-023-05268-3/FIGURES/1.

[37] L. J. Nebelsick-Gullett, T. J. Housh, G. O. Johnson, and S. M. Bauge, "A comparison between methods of measuring anaerobic work capacity," *Ergonomics*, vol. 31, pp. 1413–1419, 10 1988, ISSN: 13665847. DOI: 10.1080/00140138808966785.

[38] S. Tengattini and A. Y. Bigazzi, "Physical characteristics and resistance parameters of typical urban cyclists," *Journal of Sports Sciences*, vol. 36, pp. 2383–2391, 20 Oct. 2018, ISSN: 1466447X. DOI: 10.1080/02640414.2018.1458587.

[39] N. J. Higham, "Computing the nearest correlation matrix—a problem from finance," *IMA Journal of Numerical Analysis*, vol. 22, no. 3, pp. 329–343, 2002.

[40] CBS, *Bevolkingspiramide*, https://www.cbs.nl/nl-nl/visualisaties/dashboard-bevolking/bevolkingspiramide, (Accessed on 12/5/2024).

[41] CBS, *Cbs open data statline*, https://opendata.cbs.nl/statline/portal.html?_la=nl&_catalog=CBS&tableId=81565NED&_theme=163.

[42] M. Liu, *Optimal number of trials for monte carlo simulation*, https://mliu.org/valuation/optimal-number-of-trials-for-monte-carlo-simulation/, 2017.

A

Power and braking behaviour

In this section a part of a simulation is given in Figure A.1 to illustrate the braking behaviour of a cyclist in curves and at stops. Close to the red line, a red traffic light, the riders stops pedalling resulting in the driving power going down to zero. This is the phase between pedalling and braking. The braking force is not constant, because the speed of the cyclist and the environment change during braking. The cyclists adapts the braking force to keep a constant deceleration. In the bottom graph the curvature is plotted together with the curvature the rider looks ahead in time to, illustrated with a black dashed line. When this look ahead curvature would make the rider go over their preferred maximum lean angle the driving power drops to zero and the cyclists starts to brake. This braking continues until the point of maximum curvature is reached, at which point the look ahead curvature drops too. The driving power stays at zero for a short time after the braking has ceased, this is because the lean angle of the cyclist is at that time still above the maximum desired pedalling lean angle.

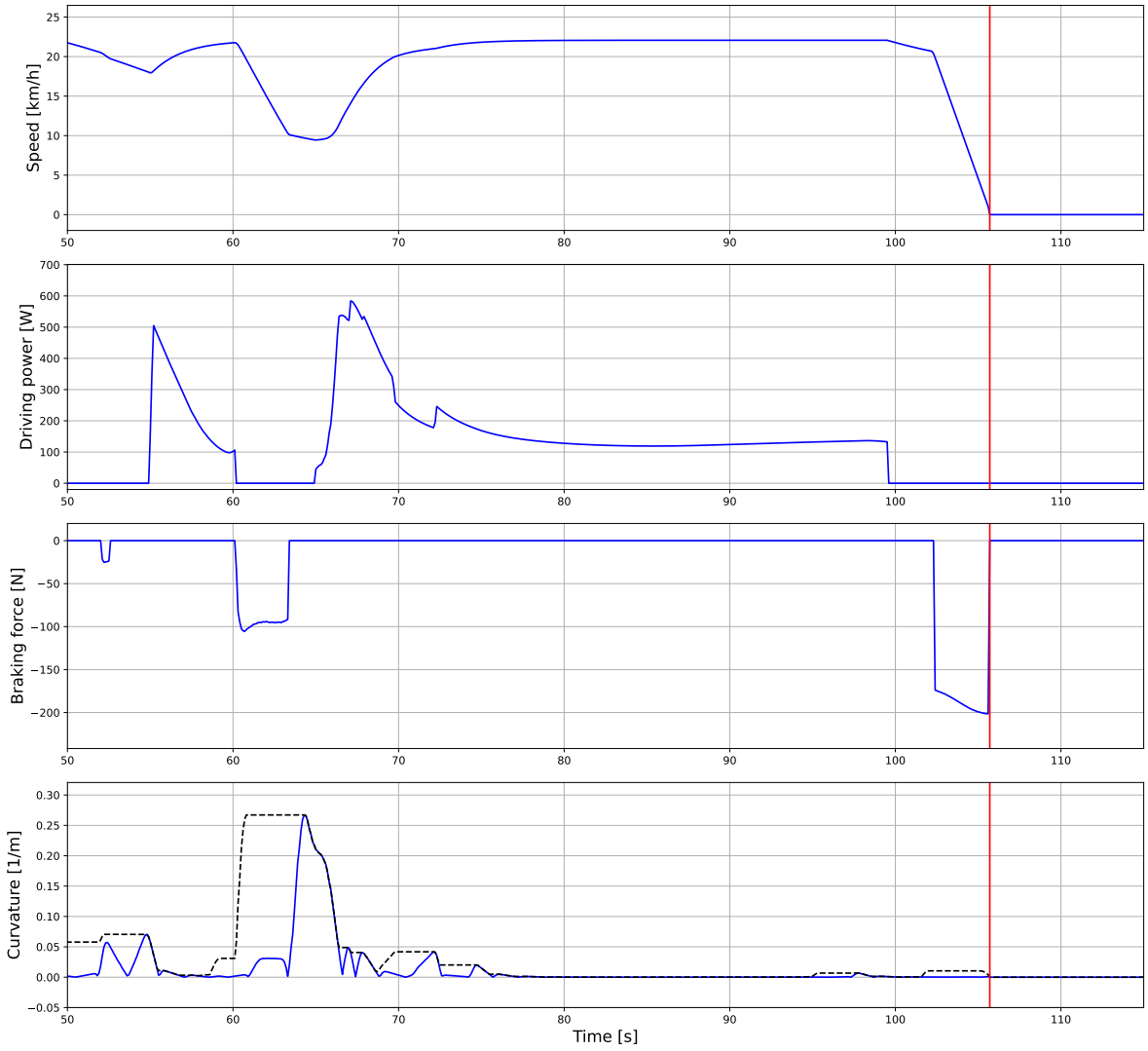

Figure A.1: Example of braking behaviour at red traffic lights, displayed as a red line, and sharp curves. The dashed black line in the curvature plot is the maximum curvature the rider looks at with the look ahead time.

B

Input data

B.1. Traffic lights data

For traffic lights, only daytime data is used, from 07:00 to 22:00 h to represent the time utility cyclist are on the road. If the model is used for a specific group, for example commuting cyclists, the rush hour times can be used to give results that reflect conditions during the time of interest. For the new traffic light on the bicycle highway there exist a bicycle traffic light in the opposite direction, this data is therefore used for the new traffic light. An overview of the chance the traffic lights is green upon arrival and the mean waiting time when it is red are given in Table B.1, the corresponding locations can be seen in Figure B.1.

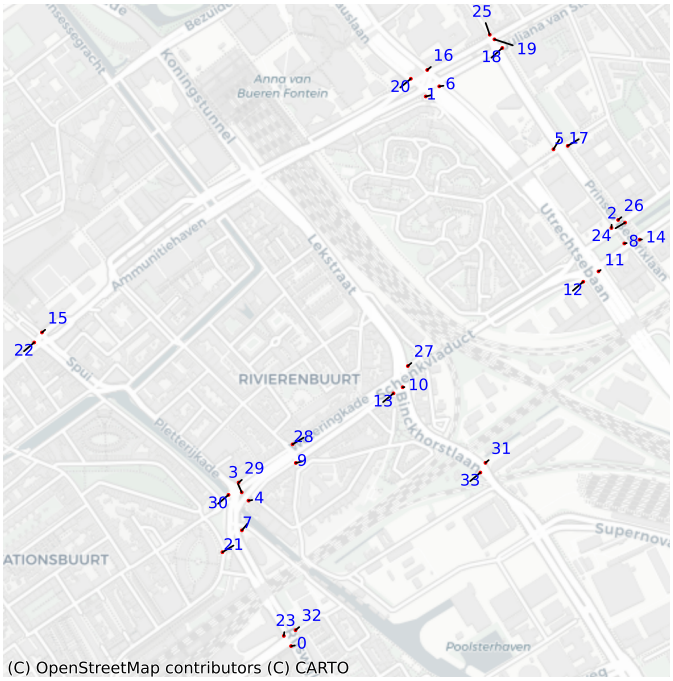

Figure B.1: Locations of all used traffic lights

	Green chance	Mean waiting time [s]
0	0.18	20.70
1	0.12	24.75
2	0.07	22.65
3	0.21	17.66
4	0.10	49.45
5	0.38	10.62
6	0.25	12.24
7	0.87	7.63
8	0.14	21.51
9	0.40	20.13
10	0.15	15.29
11	0.13	9.31
12	0.06	12.25
13	0.09	25.90
14	0.22	14.82
15	0.25	30.10
16	0.14	24.10
17	0.17	15.25
18	0.08	10.40
19	0.14	6.83
20	0.30	10.65
21	0.31	24.00
22	0.50	12.87
23	0.15	34.77
24	0.16	19.03
25	0.82	0.00
26	0.27	14.63
27	0.06	30.67
28	0.62	13.49
29	0.21	51.04
30	0.38	0.00
31	0.06	14.68
32	0.18	20.70
33	0.04	16.46

Table B.1: Chance at green light and mean waiting time at a red light for all used traffic lights

B.2. Correlations

Between many parameters used in this model a correlation can be present. To keep the amount of assumptions with a possible large effect on the model low, it is assumed that if no correlation is found between two parameters in literature they are completely independent while in reality this might not be entirely true. The only correlations found are between P_c, AWC, the age of the rider and the mass of the rider. For some parameters there is evidence that no correlation is present, while for others different sources come to different conclusions.

B.3. Elevation data

Below the elevation map made from the LIDAR data is given in Figure B.2, the flyover east route is shown as a blue line. By using the LIDAR data and removing the points classified as trees and buildings, the roads, bridges and other infrastructure remain. This LIDAR data is then converted to a coordinate based grid with a interpolation size of 0.5x0.5m that can return the elevation of any coordinate provided by obtaining the pixel elevation value at the wanted location. The elevation data obtained from the map is then further processed by removing overhead roads and other obstacles and smoothing the elevation using a b-spline of the Python $scipy.interpolate$ library with a smoothing coefficient of nine.

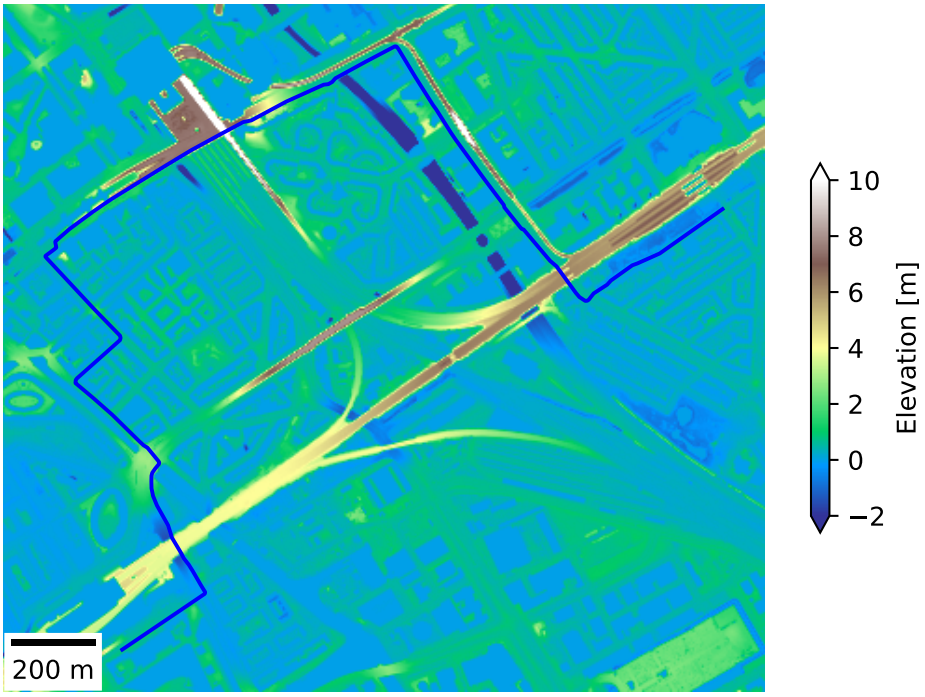

Figure B.2: The LIDAR grid with elevations on a color scale, sampled at 0.5 m by 0.5 m squares. Buildings and vegetation are set to an elevation of 0. The blue line is the flyover east route.

C

Route characteristics

Below the characteristics of all used routes are given: the type of bicycle infrastructure, position of traffic lights and give way points,and the position of the stairs in and out of the tunnel. And overview of the amount of traffic lights and give way signs together with other route data can be found in Table C.1.

Route	Length [km]	# Traffic lights	# Give way points	Elevation gain [m]	Elevation loss [m]
1	3.40	9	2	15.3	15.4
2	3.63	12	2	16.0	15.9
3	2.27	7	2	10.1	10.3
4	2.44	9	1	11.3	11.3
5	1.91	2	1	10.9	11.0
6	1.91	2	1	10.5	10.4

Table C.1: Route data overview

For the bicycle highway the length of the route and the amount of traffic lights is greatly reduced, which should have a positive impact on both the travel time and the required energy. The elevation difference however is not a clear improvement. The elevation gain and loss is significantly less than the flyover route, but very similar to that of the tunnel route with the key difference that in the tunnel route most elevation difference is covered by walking instead of cycling.

C.1. Bicycle facility types

In this section the types of bicycle infrastructure are given for each route. Most of the distance is covered by bicycle paths, and very little is shared road with cars. Still there is improvement possible as shown in Figure C.1e and Figure C.1f where no shared road or bicycle lanes are present and the bicycle is the priority vehicle on the whole route.

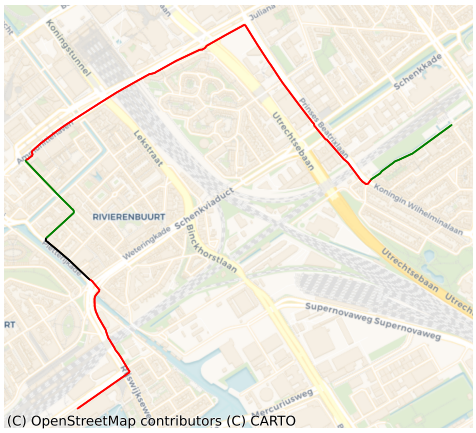

(a) Flyover east

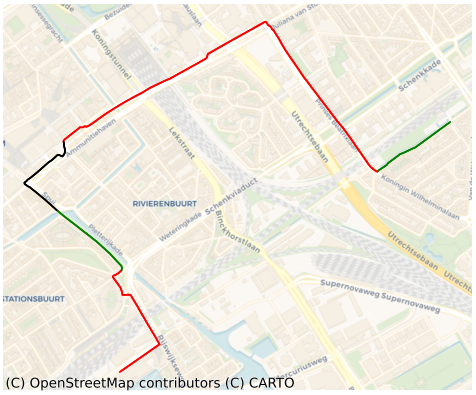

(b) Flyover west

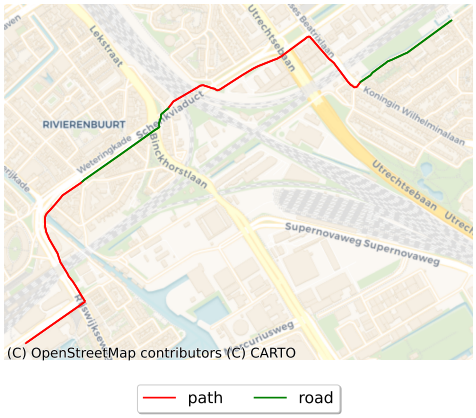

(c) Tunnel east

(d) Tunnel west

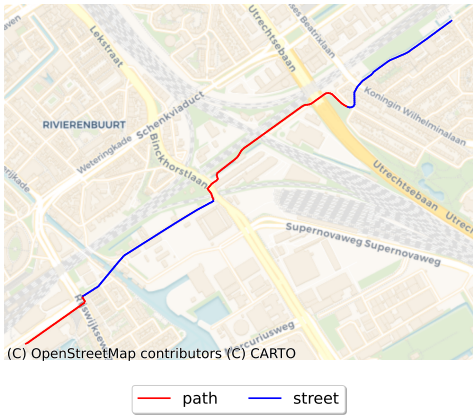

(e) Highway east

(f) Highway west

Figure C.1: Bicycle infrastructure types for all routes

C.2. Road elements

In this section an overview is given of the road elements on the routes, these include traffic lights, give way points and tunnel stairs. While the flyover routes have the most traffic lights, they are mostly present in the first and last part of the route while the lights in the tunnel routes are more spread out over the whole route.

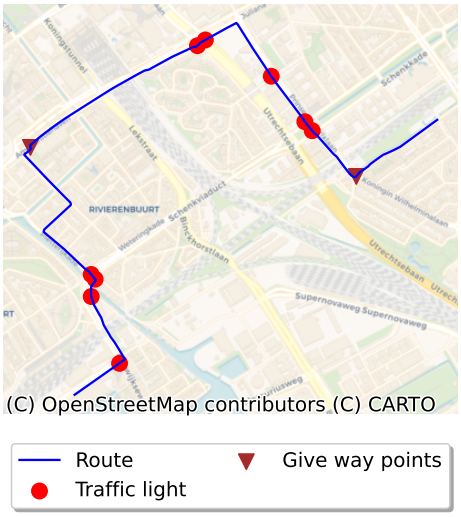

(a) Flyover east

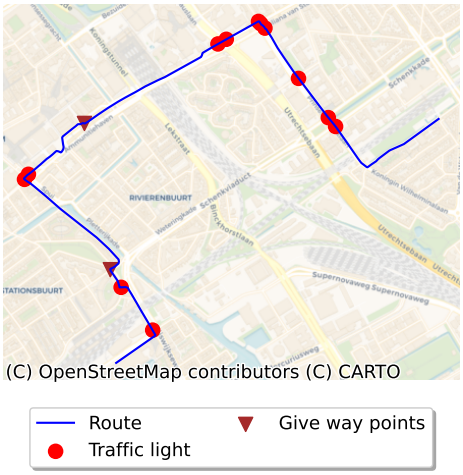

(b) Flyover west

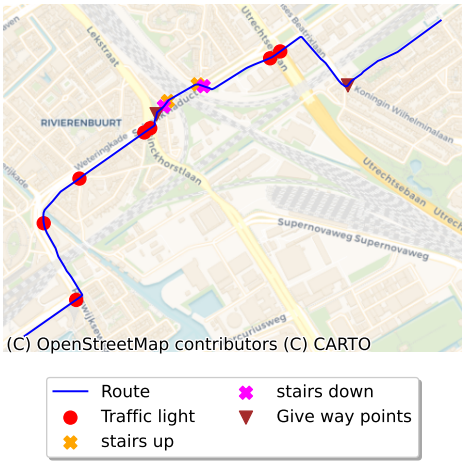

(c) Tunnel east

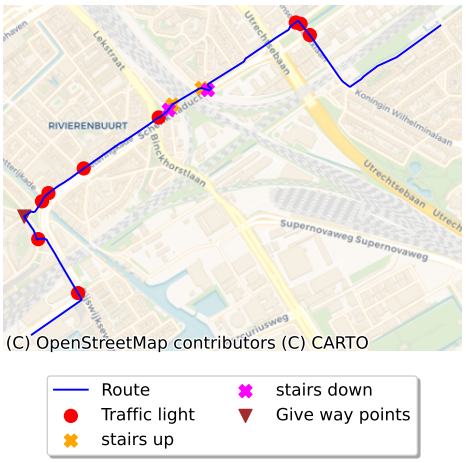

(d) Tunnel west

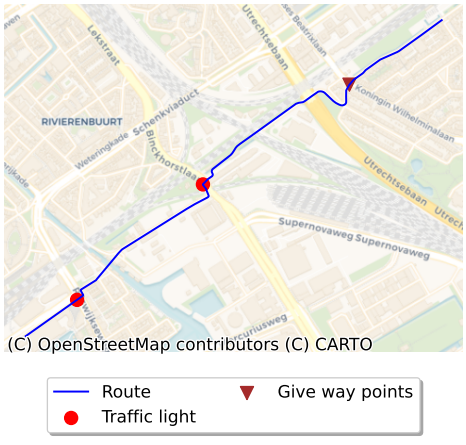

(e) Highway east

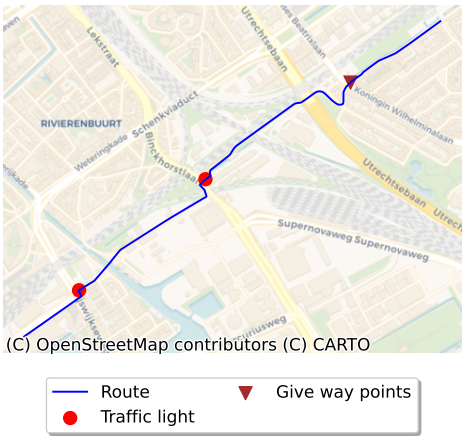

(f) Highway west

Figure C.2: Bicycle road elements for all routes

D

Results of time and energy expenditure in all routes

D.1. Time and energy distributions

Both energy and time distributions from all six routes show similar shapes. For the flyover route there is a large difference in the means of the travel time between different directions of travel, while for the highway the means are fairly close to each other. Between the results in time and energy of all routes there is a statistical significant difference, showing that all six routes give significantly different results. The highway has by far the least traffic lights the shortest distance and therefore less variability, but critically it has the same amount of traffic lights in both directions. For a complete overview of the route characteristics see Appendix C. Moreover the the distances are the exact same as the route traverses the same road, just on different sides of the bicycle path. Since there are no parts of the route around existing car infrastructure both directions of travel use the same route layout only on opposite sides of the bicycle path.

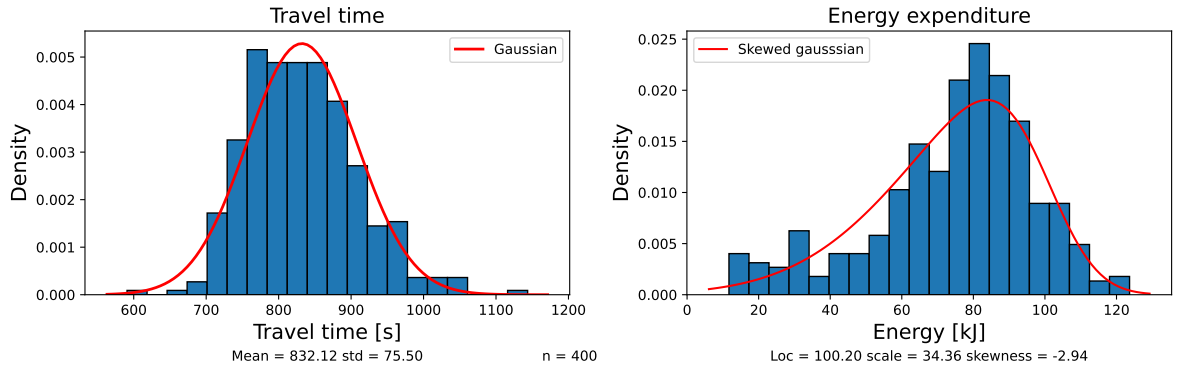

(a) Flyover east

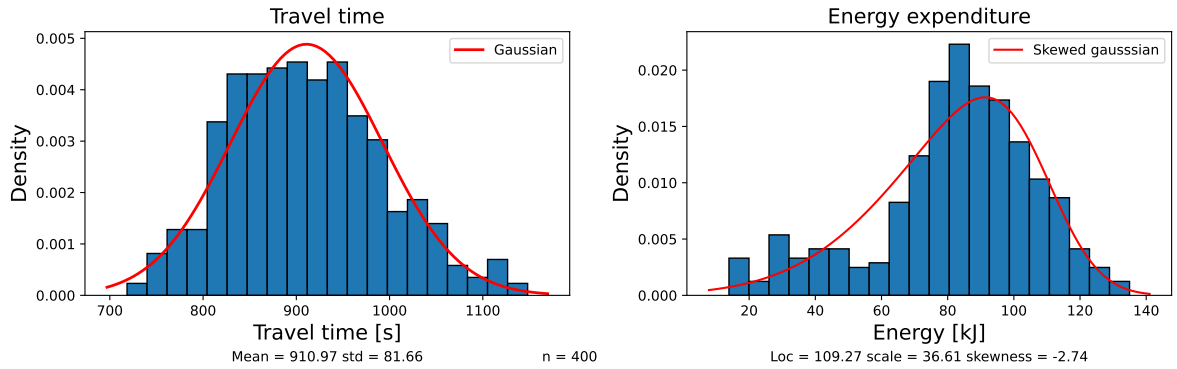

(b) Flyover west

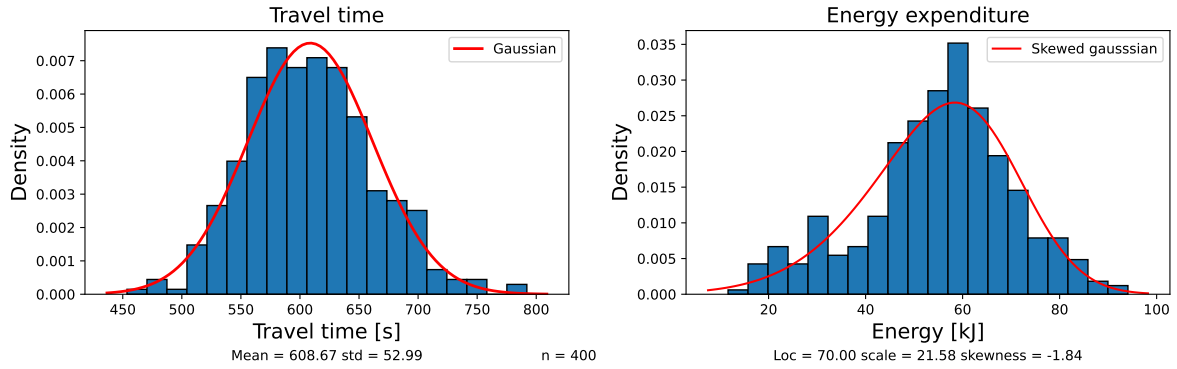

(c) Tunnel east

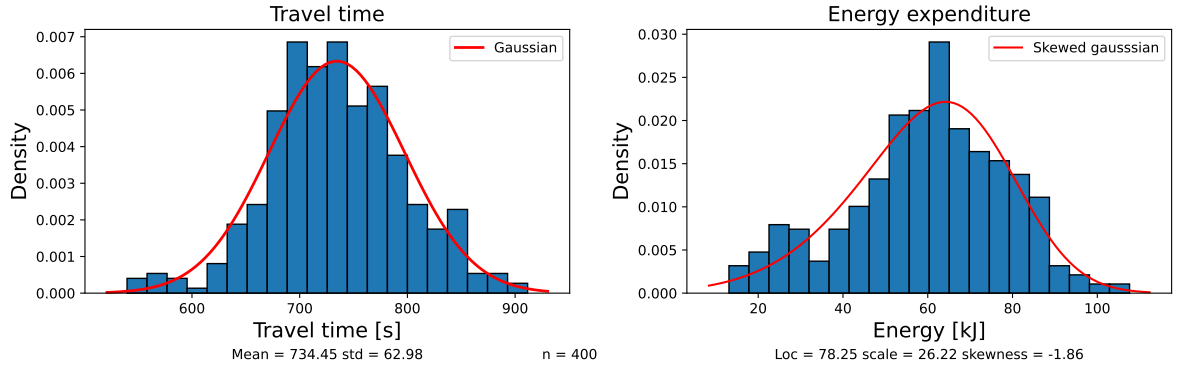

(d) Tunnel west

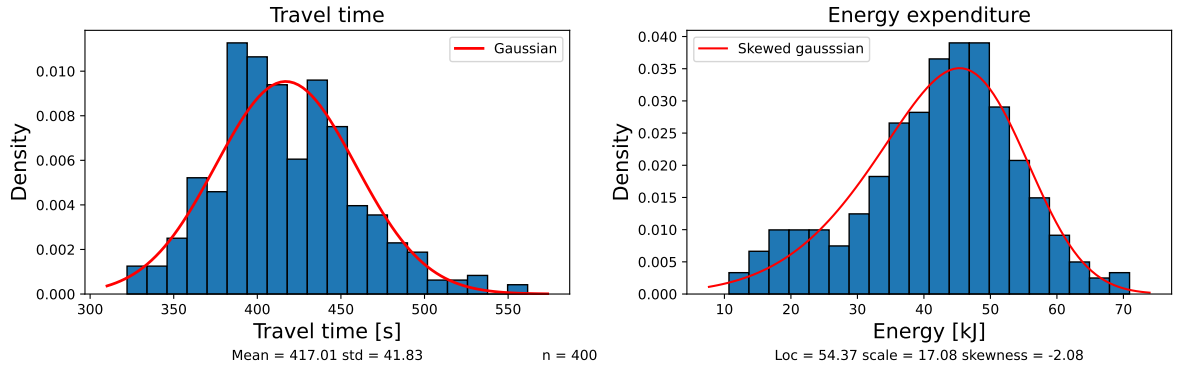

(e) Highway east

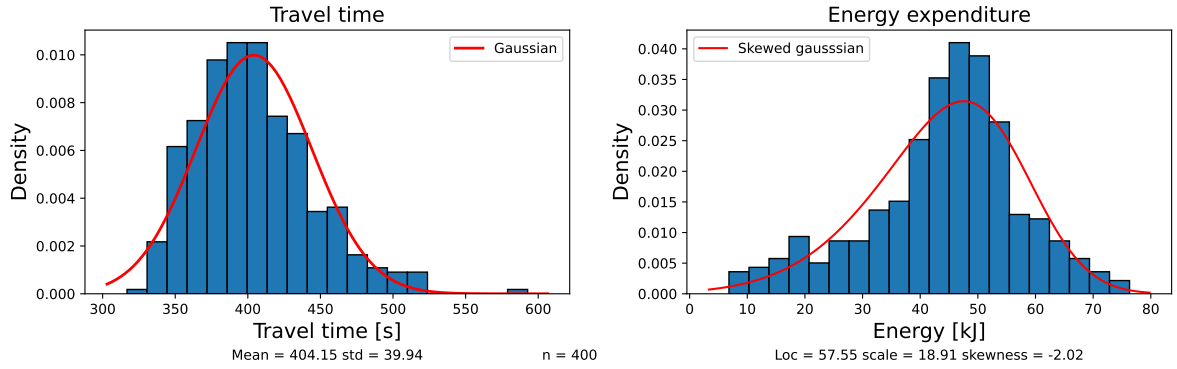

(f) Highway west

Figure D.1: Time and energy distributions of all routes with fitted Gaussian and Skewed Gaussian

D.2. Time and energy distributions split by sex

In this section all data is split into male and female categories.

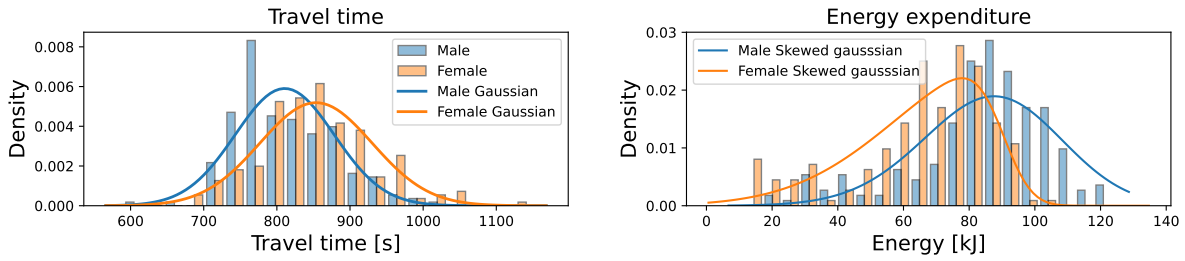

Male: Mean = 810.69 std = 67.59
Female: Mean = 853.54 std = 76.89

n = 400

Male: Loc = 100.28 scale = 25.47 skewness = -0.96
Female: Loc = 90.31 scale = 32.36 skewness = -4.67

(a) Flyover east

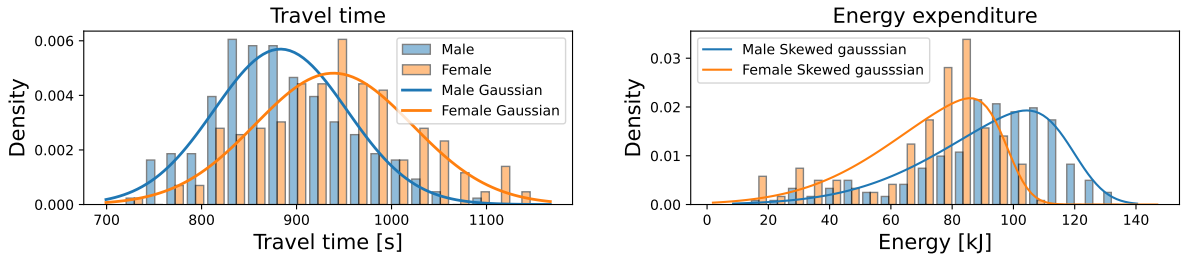

Male: Mean = 883.06 std = 70.05
Female: Mean = 938.88 std = 82.90

n = 400

Male: Loc = 119.32 scale = 36.16 skewness = -4.03
Female: Loc = 97.77 scale = 33.34 skewness = -5.31

(b) Flyover west

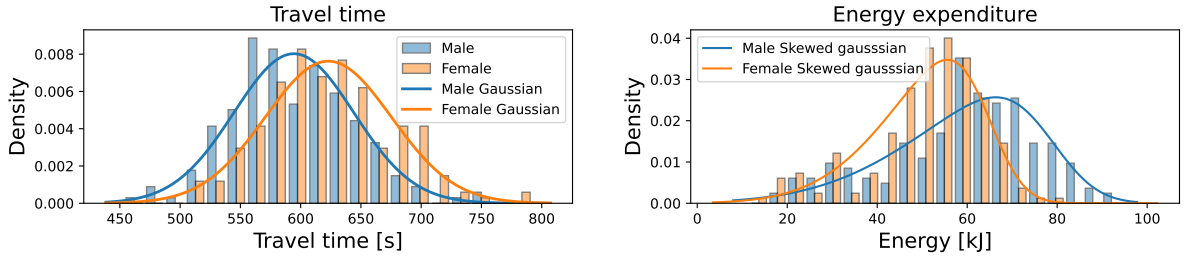

Male: Mean = 594.37 std = 49.70
Female: Mean = 622.97 std = 52.31

n = 400

Male: Loc = 78.46 scale = 25.58 skewness = -2.99
Female: Loc = 64.59 scale = 18.78 skewness = -2.91

(c) Tunnel east

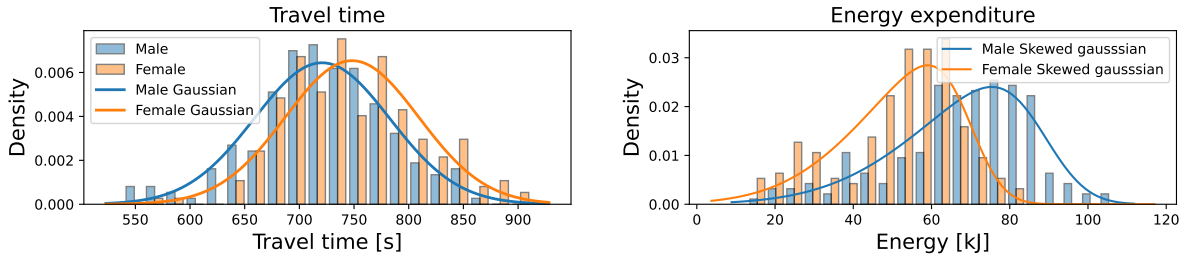

Male: Mean = 720.71 std = 61.92
Female: Mean = 748.19 std = 61.01

n = 400

Male: Loc = 88.38 scale = 27.29 skewness = -2.95
Female: Loc = 69.72 scale = 23.72 skewness = -3.39

(d) Tunnel west

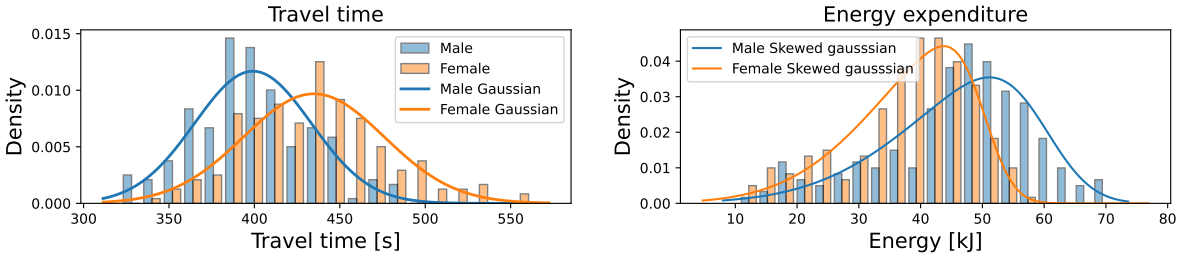

Male: Mean = 399.17 std = 34.14
Female: Mean = 434.85 std = 41.19

n = 400

Male: Loc = 59.95 scale = 18.43 skewness = -2.91
Female: Loc = 50.26 scale = 15.80 skewness = -4.09

(e) Highway east

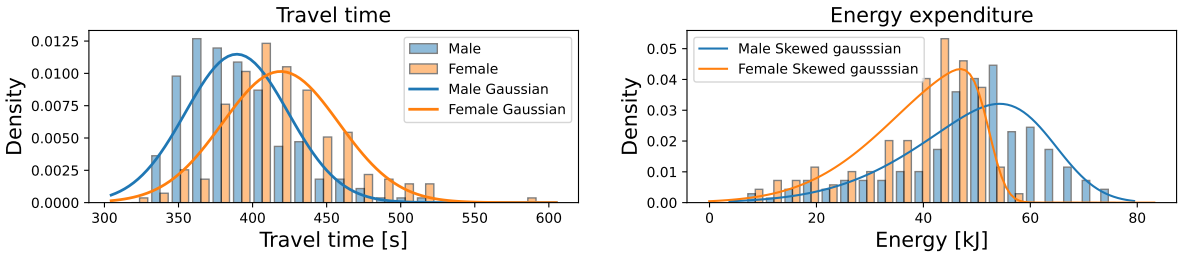

Male: Mean = 389.34 std = 34.74
Female: Mean = 418.96 std = 39.31

n = 400

Male: Loc = 64.06 scale = 20.10 skewness = -2.76
Female: Loc = 52.29 scale = 17.19 skewness = -6.68

(f) Highway west

Figure D.2: Time and energy distributions of all routes split by sex with fitted Gaussian and Skewed Gaussian

D.3. Time and energy distributions split by bicycle type

In this section all data is split into e-bike and regular bicycle users.

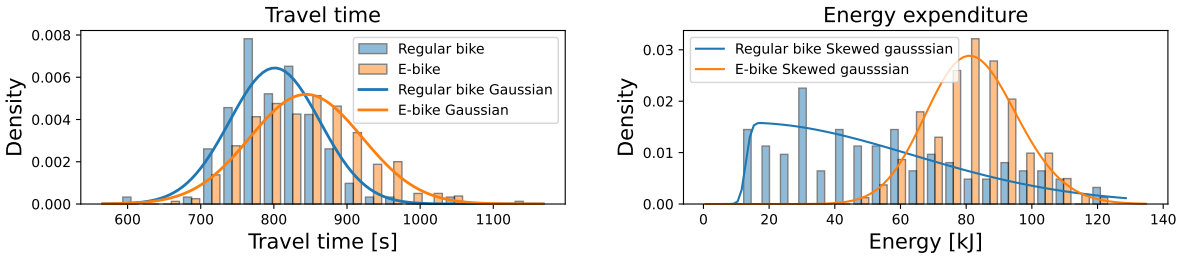

Regular bike: Mean = 801.16 std = 61.94
E-bike: Mean = 844.01 std = 76.85

n = 400

Regular bike: Loc = 12.88 scale = 50.42 skewness = 37.91
E-bike: Loc = 72.22 scale = 17.13 skewness = 1.06

(a) Flyover east

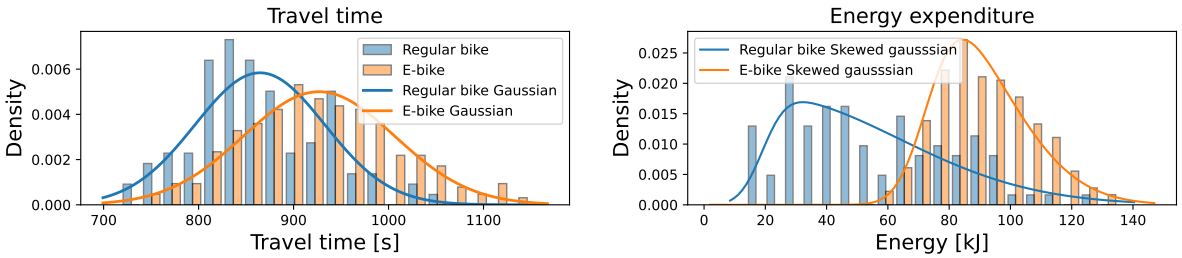

Regular bike: Mean = 864.58 std = 68.33
E-bike: Mean = 926.84 std = 79.77

n = 400

Regular bike: Loc = 19.13 scale = 44.50 skewness = 7.34
E-bike: Loc = 72.91 scale = 24.03 skewness = 2.92

(b) Flyover west

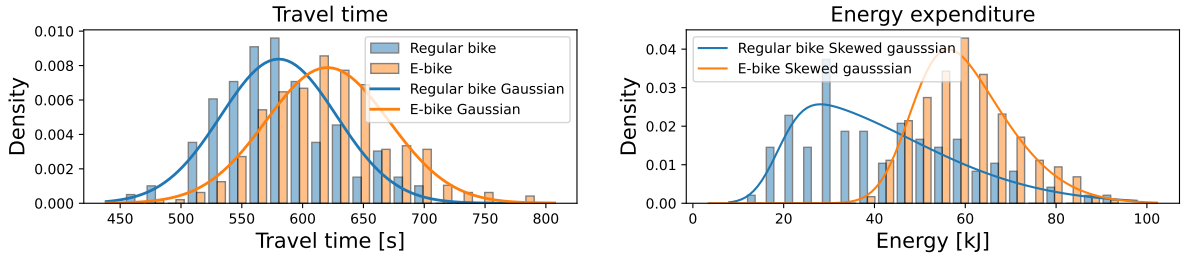

Regular bike: Mean = 580.31 std = 47.62 n = 400
E-bike: Mean = 620.40 std = 50.61

Regular bike: Loc = 18.78 scale = 28.88 skewness = 6.33
E-bike: Loc = 48.37 scale = 15.93 skewness = 2.62

(c) Tunnel east

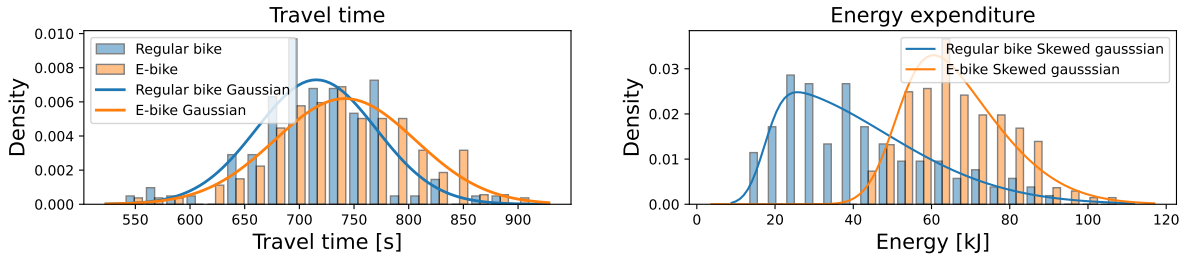

Regular bike: Mean = 715.48 std = 54.70 n = 400
E-bike: Mean = 741.74 std = 64.42

Regular bike: Loc = 17.33 scale = 30.56 skewness = 8.12
E-bike: Loc = 51.22 scale = 20.25 skewness = 3.23

(d) Tunnel west

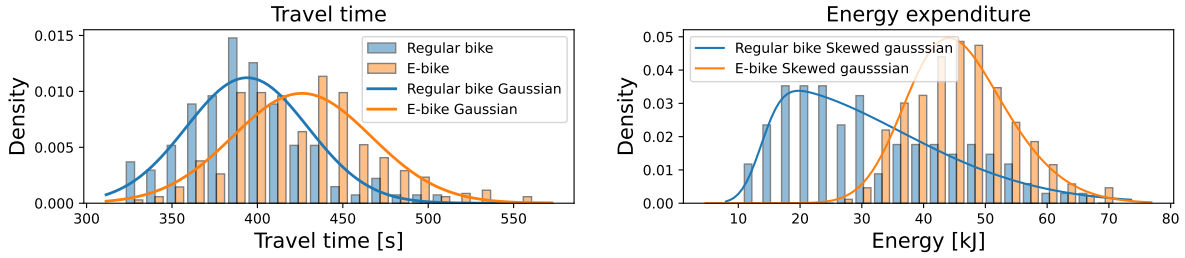

Regular bike: Mean = 393.94 std = 35.55 n = 400
E-bike: Mean = 426.09 std = 40.60

Regular bike: Loc = 13.75 scale = 22.52 skewness = 8.48
E-bike: Loc = 37.83 scale = 11.74 skewness = 1.88

(e) Highway east

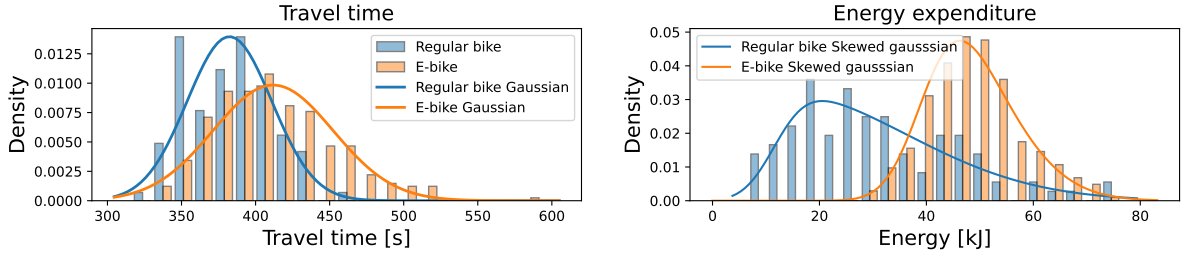

Regular bike: Mean = 382.37 std = 28.58 n = 400
E-bike: Mean = 411.80 std = 40.54

Regular bike: Loc = 11.64 scale = 24.52 skewness = 5.21
E-bike: Loc = 39.60 scale = 12.65 skewness = 2.09

(f) Highway west

Figure D.3: Time and energy distributions of all routes split by bicycle type with fitted Gaussian and Skewed Gaussian

D.4. Time and energy distributions of e-bikes split by control type

In this section the e-bike data is split between the torque and cadence control type.

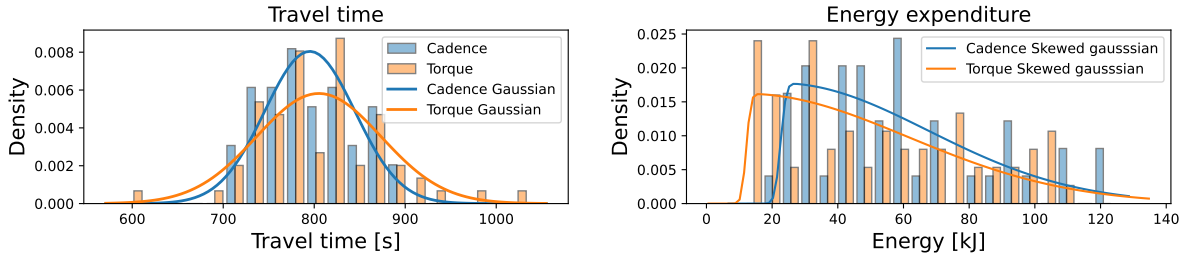

Cadence: Mean = 795.16 std = 49.60
Torque: Mean = 805.11 std = 68.56

n = 111

Cadence: Loc = 22.55 scale = 44.95 skewness = 32.98
Torque: Loc = 12.11 scale = 49.28 skewness = 44.12

(a) Flyover east

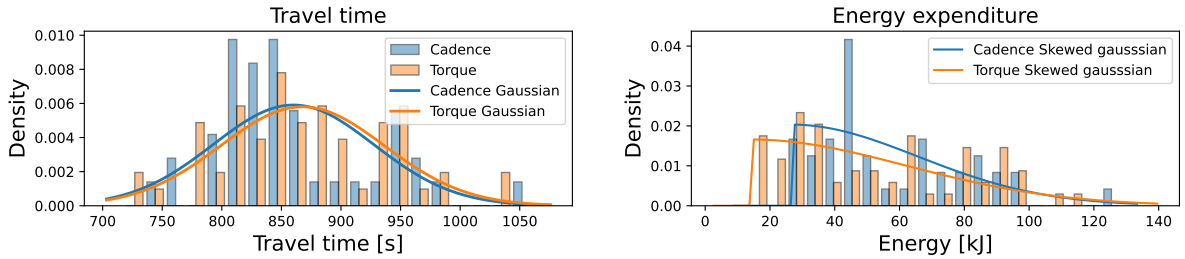

Cadence: Mean = 860.13 std = 67.51
Torque: Mean = 867.70 std = 68.73

n = 102

Cadence: Loc = 26.44 scale = 39.22 skewness = 13399000.44
Torque: Loc = 13.90 scale = 48.06 skewness = 146683729.22

(b) Flyover west

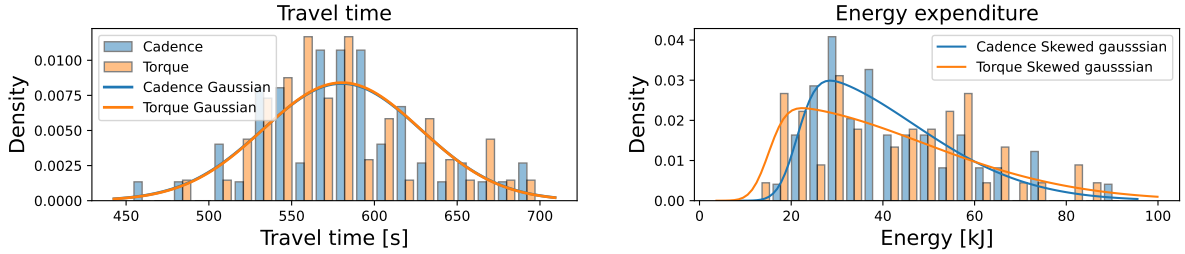

Cadence: Mean = 580.25 std = 47.78
Torque: Mean = 580.37 std = 47.46

n = 117

Cadence: Loc = 21.27 scale = 25.25 skewness = 7.64
Torque: Loc = 15.07 scale = 33.57 skewness = 11.23

(c) Tunnel east

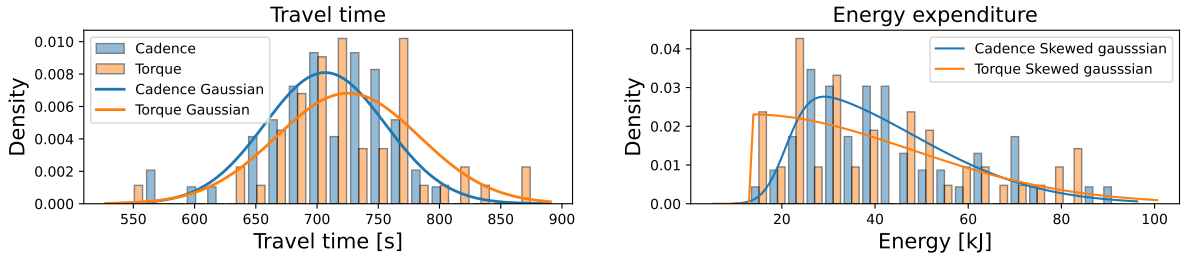

Cadence: Mean = 706.54 std = 49.29
Torque: Mean = 725.27 std = 58.52

n = 111

Cadence: Loc = 20.88 scale = 27.08 skewness = 6.96
Torque: Loc = 13.10 scale = 34.58 skewness = 70466843.51

(d) Tunnel west

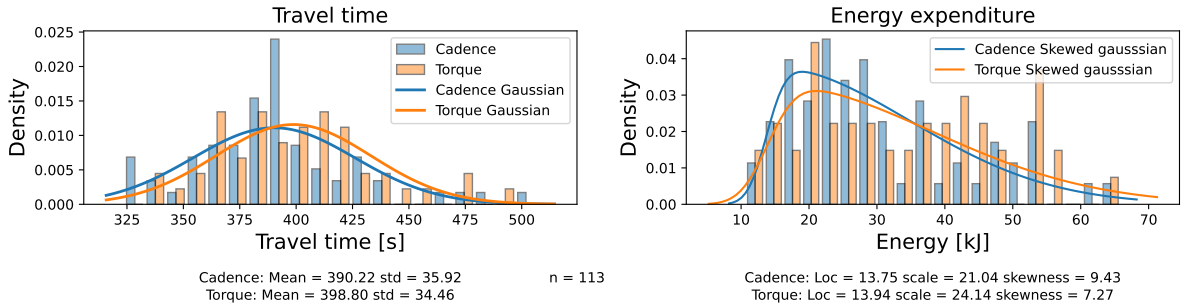

Cadence: Mean = 390.22 std = 35.92
Torque: Mean = 398.80 std = 34.46

n = 113

Cadence: Loc = 13.75 scale = 21.04 skewness = 9.43
Torque: Loc = 13.94 scale = 24.14 skewness = 7.27

(e) Highway east

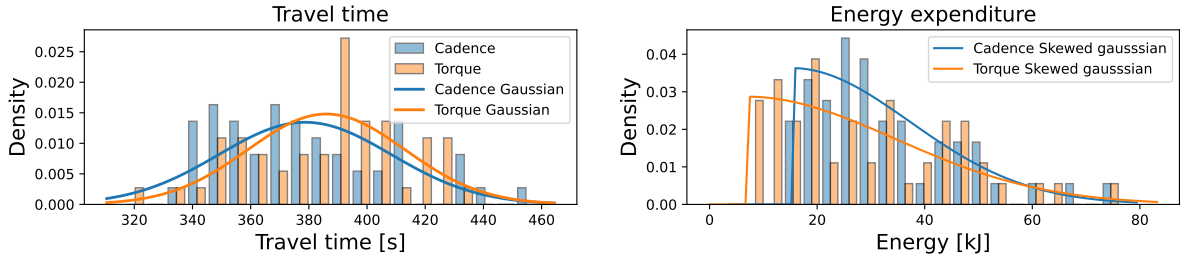

Cadence: Mean = 378.70 std = 29.67
Torque: Mean = 386.04 std = 26.95

n = 104

Cadence: Loc = 15.28 scale = 21.97 skewness = 28896029.10
Torque: Loc = 6.82 scale = 27.80 skewness = 9817129.50

(f) Highway west

Figure D.4: Time and energy distributions of all routes split by e-bike type with fitted Gaussian and Skewed Gaussian

D.5. Time and energy distributions split by age

In this section all data is split into three age categories.

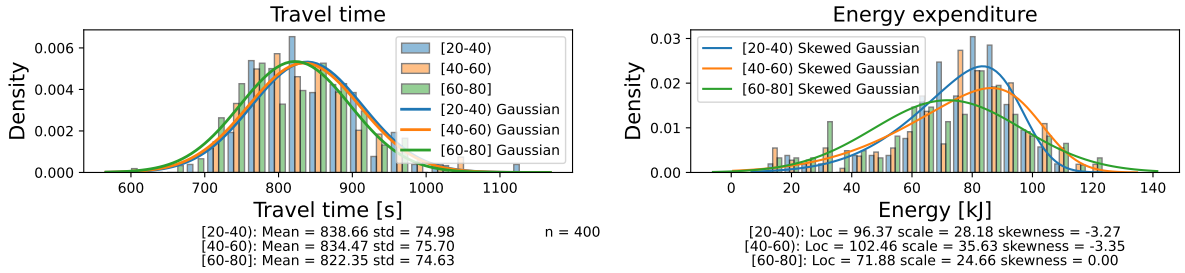

[20-40): Mean = 838.66 std = 74.98
[40-60): Mean = 834.47 std = 75.70
[60-80]: Mean = 822.35 std = 74.63

n = 400

[20-40): Loc = 96.37 scale = 28.18 skewness = -3.27
[40-60): Loc = 102.46 scale = 35.63 skewness = -3.35
[60-80]: Loc = 71.88 scale = 24.66 skewness = 0.00

(a) Flyover east

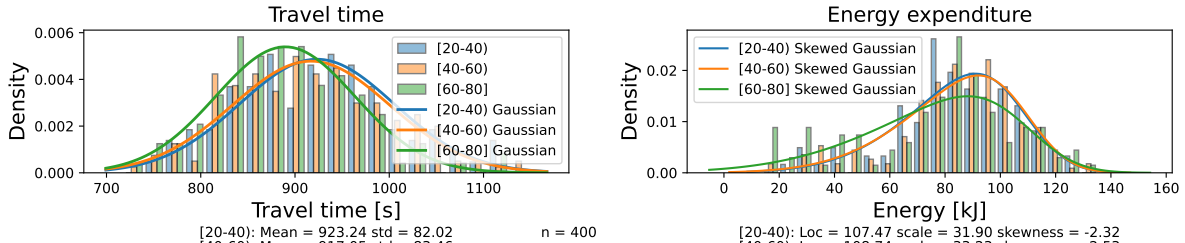

[20-40): Mean = 923.24 std = 82.02
[40-60): Mean = 917.05 std = 83.46
[60-80]: Mean = 889.74 std = 73.97

n = 400

[20-40): Loc = 107.47 scale = 31.90 skewness = -2.32
[40-60): Loc = 108.74 scale = 33.23 skewness = -2.53
[60-80]: Loc = 109.15 scale = 43.53 skewness = -2.87

(b) Flyover west

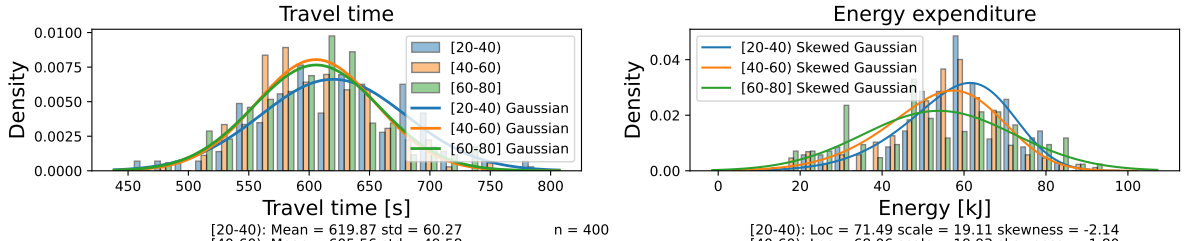

[20-40): Mean = 619.87 std = 60.27
[40-60): Mean = 605.56 std = 49.58
[60-80]: Mean = 605.84 std = 52.11

n = 400

[20-40): Loc = 71.49 scale = 19.11 skewness = -2.14
[40-60): Loc = 68.06 scale = 19.93 skewness = -1.80
[60-80]: Loc = 53.85 scale = 18.49 skewness = 0.00

(c) Tunnel east

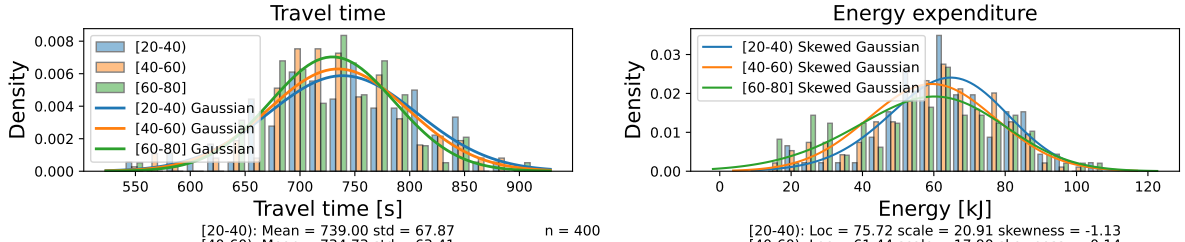

[20-40): Mean = 739.00 std = 67.87
[40-60): Mean = 734.73 std = 63.41
[60-80]: Mean = 729.63 std = 56.72

n = 400

[20-40): Loc = 75.72 scale = 20.91 skewness = -1.13
[40-60): Loc = 61.44 scale = 17.90 skewness = -0.14
[60-80]: Loc = 75.01 scale = 27.49 skewness = -1.34

(d) Tunnel west

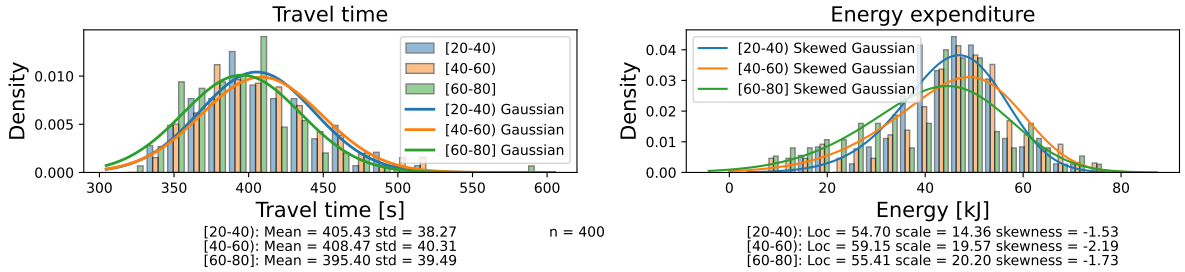

(e) Highway east

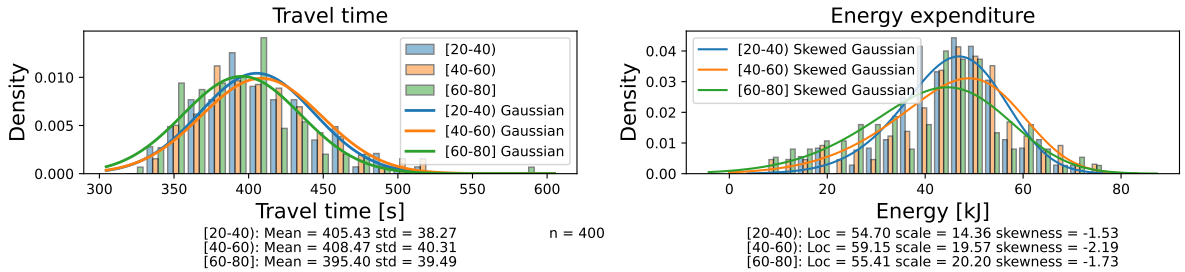

(f) Highway west

Figure D.5: Time and energy distributions of all routes split by age with fitted Gaussian and Skewed Gaussian

D.5.1. Significance tests

In Table D.1 the results of Kruskal-Wallis tests are shown. For the age split data a post hoc test is performed, see Table D.2.

		Category	**Sex**	**Age**	**Bicycle type**	**E-bike control**
Direction	**Route**	**Groups compared**	**Male Female**	**20-40 40-60 60-80**	**E-bike Regular**	**Torque Cadence**
East	**Flyover**	Time	<.000***	.366	<.000***	.430
		Energy	<.000***	.323	<.000***	.185
	Tunnel	Time	<.000***	..076	<.000***	.752
		Energy	<.000***	.124	<.000***	.690
	Highway	Time	<.000***	.043*	<.000***	.156
		Energy	<.000***	.086	<.000***	.207
West	**Flyover**	Time	<.000***	.005**	<.000***	.384
		Energy	<.000***	.075	<.000***	.180
	Tunnel	Time	.009**	.458	<.000***	.194
		Energy	<.000***	.174	<.000***	.479
	Highway	Time	<.000***	.021*	<.000***	.078
		Energy	<.000***	.056	<.000***	.125

Table D.1: The p-values for different input parameters in the model with given significance levels.
* $p < .05$
** $p < .01$
*** $p < .001$

				[20-40)	[40-60)	[60-80]
East	Flyover	Time	[20-40)	-	.635	.529
			[40-60)	.635	-	.548
			[60-80]	.529	.548	-
		Energy	[20-40)	-	.862	.862
			[40-60)	.862	-	.398
			[60-80]	.862	.398	-
	Tunnnel	Time	[20-40)	-	.082	.146
			[40-60)	.082	-	.862
			[60-80]	.146	.862	-
		Energy	[20-40)	-	.154	.179
			[40-60)	.154	-	.991
			[60-80]	.179	.991	-
	Highway	Time	[20-40)	-	.727	.076
			[40-60)	.727	-	.076
			[60-80]	.076	.076	-
		Energy	[20-40)	-	.088	.496
			[40-60)	.088	-	.496
			[60-80]	.496	.496	-
West	Flyover	Time	[20-40)	-	.499	.009**
			[40-60)	.499	-	.013*
			[60-80]	.009**	.013*	-
		Energy	[20-40)	-	.727	.209
			[40-60)	.727	-	.078
			[60-80]	.209	.078	-
	Tunnnel	Time	[20-40)	-	.897	.636
			[40-60)	.897	-	.897
			[60-80]	.636	.897	-
		Energy	[20-40)	-	.371	.194
			[40-60)	.371	-	.420
			[60-80]	.194	.420	-
	Highway	Time	[20-40)	-	.639	.095
			[40-60)	.639	-	.019*
			[60-80]	.095	.019*	-
		Energy	[20-40)	-	.666	.183
			[40-60)	.666	-	.055
			[60-80]	.183	.055	-

Table D.2: The p-values for different age groups with given significance levels based on a post hoc analysis

* $p < .05$

** $p < .01$

*** $p < .001$

E

Traffic lights

E.1. Impact on time and energy

In this section the impact of traffic lights for all routes is displayed by the difference in mean energy and time compared to the mean of the whole sample. In all cases the time gained increases as the amount of green lights increases, while the time fluctuates. Due to the limited amount of samples per green light category the results show no clear relation between the amount of green lights and the travel energy cost. With more simulations it is expected that the energy will reduce with more green lights in the same manner as the travel time, because it will matter less which light is turned green when a higher amount of samples is used. On the new highway route only two traffic lights are present resulting in larger sample rates per category as the data points are divided over less categories. In both directions a clear reduction in both travel time and energy expenditure can be observed. With more data samples the average time and energy saved by removing a traffic light can be found, when going even further and splitting the data per individual traffic light the impact of a single light can be observed.

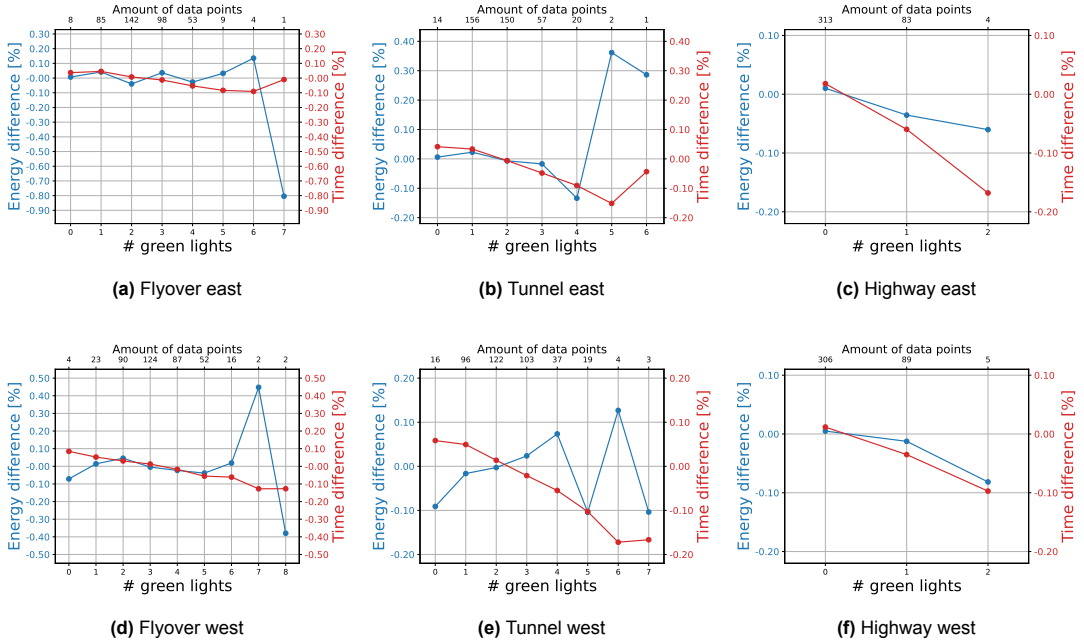

(a) Flyover east **(b)** Tunnel east **(c)** Highway east

(d) Flyover west **(e)** Tunnel west **(f)** Highway west

Figure E.1: The effect of traffic lights on energy and time

F

Sensitivity analysis

There are many inputs in the model that can make a difference in the output of time and energy, to see how much of a impact each parameter has a sensitivity analysis is performed on the tunnel route in west direction by increasing each variable by 5% one at a time, see Table F.1. These values can give an indication of what variables are most important to get realistic values of, for example a 5% increase int the mass of the rider will result in 2.22% more energy that is required, showing that rider mass is an important factor. Another major factor is the drivetrain efficiency resulting in a decrease in required energy of 2.41 % while the original efficiency was already well over 90 %. The possible gains in drivetrain efficiency are relatively low as it can't go over 100 % and is usually above 90 %, but even small improvements can lead to big differences in energy requirement. Another interesting result is that an increase in critical power will, as expected, lead to a time gain. The percentage of extra energy requirement however, is more than twice as high as the air resistance will increase with the speed squared. The AWC has no impact on either of the outputs, this is likely due to all cyclist starting with a full capacity and the routes not being long enough to drain much energy resulting in lower possible power outputs. With lower AWC values or less than full starting capacities the results could be very different. When the AWC is set to zero, the route time is 1.61 % slower showing that AWC does have an impact, but only at lower values for the tested routes.

For e-bikes it is noticeable that the total energy usage goes down drastically, while the time gain is much lower. This is likely due to the way the comfort speed is calculated in the model, it takes the e-bike power into account but doesn't go over 25 km/h unless the cyclist would have a comfort speed over 25 km/h without the e-bike power. This is done to ensure a smooth power output, if the cyclist would try to reach a speed where the e-bike motor would turn off he would slow down above this speed and the motor would turn on again after the speed has dropped below the activation speed leading to the speed going over the activation speed again. This would result in fluctuations in the motor power as the e-bike motor would turn on and off consistently while the speed is fluctuating around the activation speed. The same reasoning about comfort speed would explain the fact that all e-bike simulations result in the same relative time difference.

The only variable change leading to no differences in energy and time is the downhill speed, because the maximum speed reached on this route is below the safety speed. There are no downhill sections in the tunnel route, and because of the lack of mountains in the Netherlands this would likely be a sparely used feature in Dutch cycling models.

Variable	Base value	New value (+5%)	Unit	Route Time [min:sec]	Energy Usage [kJ]	Route Time Difference [%]	Energy Usage Difference [%]
Baseline	-	-	-	10:13	72.15	0.00	0.00
mass bike	16.00	16.80	kg	10:13	72.33	-0.01	0.25
mass rider	84.40	88.62	kg	10:15	73.75	0.21	2.22
c_r	0.0077	0.0088	-	10:16	72.35	0.37	0.28
$c_d A$	0.559	0.587	m^2	10:16	72.29	0.50	0.20
ρ	1.20	1.26	kg/m^3	10:16	72.29	0.50	0.20
$v_{downhill}$	9.72	10.21	m/s	10:13	72.15	0.00	0.00
$\eta_{drivetrain}$	0.915	0.961	-	10:08	70.41	-0.90	-2.41
P_c	0.655	0.688	-	10:08	73.59	-0.90	1.99
$a_{braking}$	1.5	1.575	m/s^2	10:12	72.30	-0.19	0.20
ϕ_{max}	12.5	13.125	Degrees	10:11	72.13	-0.42	-0.03
a_{max}	0.7	0.735	m/s^2	10:11	72.47	-0.42	0.45
t_{ahead}	2.0	2.10	s	10:15	71.77	0.19	-0.53
AWC	16150	16957.50	J	10:13	72.15	0.00	0.00
v_{stop}	0.594	0.624	m/s	10:13	72.13	-0.02	-0.03
e-bike mode	None	Cadence	-	09:47	30.99	-4.33	-57.05
e-bike mode	None	Torque	-	09:47	53.84	-4.33	-25.38
assist level (torque)	0.60	0.80	-	09:47	48.62	-4.33	-32.61
assist level (cadence)	0.60	0.80	-	09:47	22.83	-4.33	-68.36

Table F.1: Sensitivity analysis of route 4

G

Stop speed

If the braking detection point with a time step of 0.1 s is taken one step to late with a speed of 20 km/h, the braking distance offset is 0.56 m. Together with a constant deceleration of 1.5 m/s^2 the speed offset at the stop point is 4.67 km/h. Because the solver uses an iterative time step the error is not deterministic. To solve this problem the stop speed of all cyclists is set at 0 km/h and the stopping speeds are compared with the true speeds in Figure G.1, where it can be seen that the distributions have similar range and shape. The main resulting difference in the model is that with the true speeds a cyclist will always stop at the same speed, while with the adaptation the stopping speed is different for different points and the same cyclist. This doesn't necessarily reduce the validity of the model as cyclists will likely not step off their bike at the same speed every time. Also when looking at the sensitivity analysis in Appendix D , the stop speed has little to no impact on either the total travel time or energy expenditure. The error can be avoided by setting stricter integration tolerances, in that case the true distribution of stopping speeds can be used.

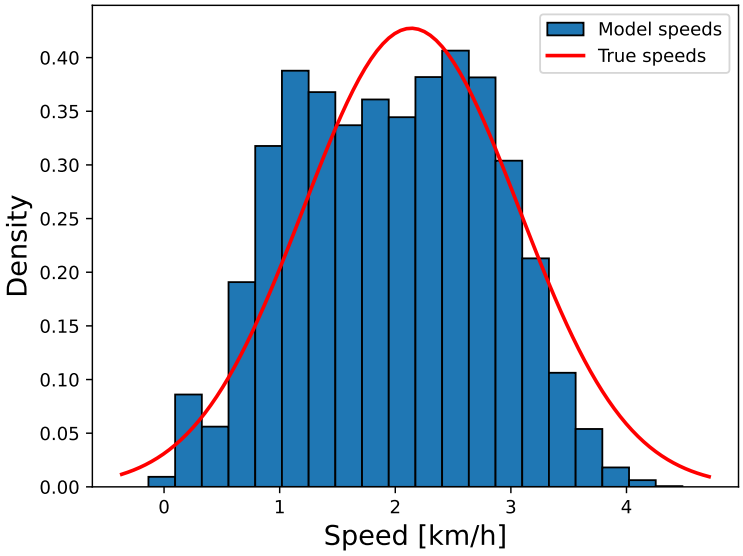

Figure G.1: Comparison of model stop speeds and true stop speed distribution